LAND COVER AND LAND USE CHANGES UNDER FOREST PROTECTION AND RESTORATION IN TIANTANGZHAI TOWNSHIP, ANHUI, CHINA

Qi Zhang

A thesis submitted to the faculty of the University of North Carolina at Chapel Hill in partial fulfillment of the requirements for the degree of Master of Arts in the Department of Geography.

Chapel Hill
2014

Approved by:

Conghe Song

Xiaodong Chen

Lawrence Band

ABSTRACT

QI ZHANG: Land Cover and Land Use Changes under Forest Protection and Restoration in Tiantangzhai Township, Anhui, China (Under the direction of Conghe Song)

Deforestation and forest regeneration are two key changes in the forest ecosystem that have profound impacts of the goods and services in terrestrial ecosystem. In late 1990s, China implemented Sloping Land Conversion Program (SLCP) and Natural Forest Protection Program (NFPP) aimed at forest protection and restoration. Using archived historical images, this study compared the land-cover/land-use (LCLU) changes before and after the programs and developed remote sensing indices to characterize the growth trajectory of "Grain-For-Green" (GFG) and natural forests. The results indicate substantial increase of natural forest cover during 2002-2013, compared with that during 1992-2002. The proposed indices revealed aggradation for both NFPP and GFG forests since the implementation of these policies. Further analysis found spatial variation of forest development depends on the topographic factors. This study reveals that SLCP and NFPP have been improving forest growth and development in the study area since the implementation of these policies.

ACKNOWLEDGEMENTS

I take this opportunity to express my profound gratitude and deep regards to my advisor, Dr. Conghe Song, for his exemplary guidance, monitoring and constant encouragement throughout the course of this thesis. I offer my sincere appreciation for the learning opportunities provided by Dr. Lawrence Band and Dr. Xiaodong Chen for their advices throughout the research.

My completion of this project could not have been accomplished without the support my research group members: Matthew Dannenberg, Yulong Zhang, Chris Hakkenberg and Chong Liu. The discussions with them provides me with great thoughts in processing remote sensing data and interpretation of results. Thanks also to the support of Matthew J. Burbank summer research fellowship from graduate school of UNC, which provided me the opportunity for data collection during summer 2013.

I am also deeply grateful to my parents for their help and guidance for my life. Their valuable and constructive suggestions shall carry me a long way in the journey of life on which I am about to embark.

TABLE OF CONTENTS

LIST OF TABLES

Table

LIST OF FIGURES

Figure

1. INTRODUCTION

Land cover and land use (LCLU) change is the main driver of the habitat fragmentation that resulted changes in essential goods and services provided by the terrestrial ecosystem (Butchart et al., 2010; Millennium Ecosystem Assessment, 2005; Fischer et al., 2012; Sieber et al., 2013). LCLU change is sensitive not only to the changes in environmental conditions but also to human activities. The spatiotemporal dynamics can significantly modifies the energy exchanges between the Earth's surface and atmosphere and therefore the feedback to the society supporting human beings (Otterman 1974; Charney and Stone 1975; Sagan et al. 1979). It is reported that land cover at global scale has been transformed under the human use of land resources including agricultural cultivation, pasture exploitation, forest harvesting, build-up constructions, and the like (Meyer, 1995; Dale et al., 2000). As the global population rapidly grows, land use activities also alter the landscape structures by introducing new land cover types which has substantial impacts on the natural habitats for existing endemic species (Turner et al., 2001). One of the major changes caused by human activities involving forest cover includes two fundamental types: deforestation and regeneration (Song et al., 2002; Song et al., 2007). Over decades, forests has been suffering critical loss particularly in developing countries for agricultural expansions, which posed high threats to the environment and caused ecosystem degradation (Dobson et al., 1997; Salim and Ullsten, 1999). Forests are also believed to play crucial role in global carbon sequestration (Dixon et al., 1994; Pan et al., 2011) and recent studies suggested the trend of

forest regrowth may be the major reason for the "missing sink" of carbon budgets (Caspersen et al., 2000; Myneni et al., 2001; Lelieveld, 2010).

The over-exploitation of forest resources in China caused various problems to the natural environment in terms of the sustainable development at national scale. After a half-century forest logging policy, China experienced disastrous droughts in 1997 and floods in 1998, following which the central government implemented a new protection program called Natural Forest Protection Project (NFPP) in 1998. This new policy was regarded as the largest logging-ban program in the world, aimed at forest conservation and protection from forest degradation, biodiversity loss and soil erosion (Zhang et al., 2000; Mullan et al., 2010; Zheng et al., 2011). Depending on priority levels, the households living in policy-implemented regions receive different levels of financial support by central government for managing natural forests without timber harvesting. To expand the existing conservation of forest ecosystems, China in 2001 has also adopted forest restoration program which encouraged households to convert their cropland to the forests. These participating lands are located mainly on steep slopes with low productivity or even abandoned by the farmers. Therefore, the restoration program is called Sloping Land Conversion Program (SLCP), also known as "Grain-for-green" program. This program involves a scheme of payment for ecosystem service (PES) which provides financial support for the participated household based on the area of converted land to compensate the loss of income from the croplands. A secondary goal is to alleviate poverty of local farmers (China State Council, 2000; Chen et al., 2012; Vina et al., 2013; Song et al., 2013). As a result of the forest conservation and restoration, the major source of income for local residents has gradually changed from

harvesting wood and farming work to non-farming labor work except for the compensation by government support.

The forest programs were evaluated in several provinces of China by researchers and were believed to be effective for the conversion of marginal cropland to forests as well as providing financial support to households in poor areas (Wang et al., 2007; Gauvin et al., 2010; Chen et al., 2010). However, some researchers have reported that China's preliminary work on logging bans and forest restoration programs have mixed success with various limitations which may not be adequate tools for forest management (Durst et al., 2001; CIFOR REHAB, 2003; WRI, 2003). Many studies also indicated that the performance of the programs varies strongly depending on different local context (Persha et al., 2011; Song et al., 2013) and there is limited research particularly on tracking growth trend of the regenerated forests. There is also concern that the re-conversion from forest or grassland to cropland and wood harvest of natural forest would be possible if government subsidies were stopped (Hu et al., 2006; Shen et al., 2006).

Due to the complexity of synergistic effects on the local environment, more extensive and sophisticated experiments of the forest conservation and rehabilitation programs at local scale are required for better understanding their influence as well as feedbacks from ecosystems before scaling up for nationwide policy implementations (Weyerhaeuser et al., 2005). Advanced tools such as satellite images offer the opportunity to comprehensively monitor the growth trend of the natural forest and converted forests and thus to offer timely feedback for the improvement of large programs (Liu et al., 2008). Remote sensing allows useful approaches in mapping land cover at large scales both spatially and temporally. For example, Landsat images with multiple dates can be used to detect the temporal change given

one large area while high spatial resolution remotely sensed data such as WorldView-2 images can be used to evaluate the effectiveness of forest cover observation with detail information. In addition, the combination of remote sensing and GIS serves as a powerful tool in analyzing the landscape pattern of the earth surface (Serra et al., 2008; Geri et al., 2010). Landscape ecological concepts and metrics offers fundamental theories for better understanding of sustainability of land use planning by the applications of landscape transformation (Leritão and Ahern, 2002; Ribeiro and Lovett, 2009).

In contrast to the conversion of forest to cultivated land, forest regeneration due to policy implementation pertains much to the study of forest at their early stages with remotely sensed data (Song and Woodcock, 2002). The land cover changes regarding forest successional stages can be of significance to the global carbon cycling and conservation of water resources (Woo et al., 1997; Chen et al., 2002; Preditzer and Euskirchen, 2004). It is also believed that mapping regenerated forest is much more challenging than mere deforestation due to the difficulty of monitoring the gradual changes of forest succession particularly after canopy closure (Pax-Lenney et al., 2001; Song et al., 2007). Several researchers have devoted efforts to characterize the spectral response of the forests at different successional stages with remotely sensed imageries. The Tasseled-Cap Transformation (Kauth and Thomas, 1976), which linearly converts spectral signals of Landsat Satellite data into meaningful measures of brightness, greenness and wetness, has proven to be informative in separating young, mature and old-growth forests (Cohen et al., 1995; Fiorella and Ripple, 1993a). Fiorella and Ripple (1993b) also found a high correlation between the “structural index” (TM 4/5 ratio) and the age of Douglas-fir stands which can be used to distinguish poorly regenerated forests from those that regenerated well.

However, the applications of empirical relationships with single date image by previous studies are limited due to the high dependence of extraneous factors in terms of local environmental context (Gemmell, 1999; Gemmell and Varjo, 1999). It is suggested in several papers that multiple images at various dates should be incorporated to identify the distribution of forest at different successional stages (Helmer et al., 2000; Lucas et al., 2002). Song et al (2002) characterized the spectral temporal trajectories for early successional forests and found several sources of noise such as topography and initial background conditions could potentially prevent accurate estimate of forest successional stages. The uncertainties caused by topography, atmospheric condition, phenology and sun/view angles were further evaluated (Song and Woodcock, 2003; Millan et al., 2013) and the results indicated that Tasseled Cap indices as well as normalized difference vegetation index (NDVI) of forests at different stage can be affected by these factors. Song et al. (2007) simulated the spectral reflectance of forest successions and used regression analysis to fit the successional trajectories for spectral predictors of Tasseled Cap transformation. The results showed that the brightness and greenness performed much better than wetness index for successional forests and also emphasized the monitoring effectiveness of using multitemporal Landsat imagery based on regression analysis. Overall, more efficient approaches are required to capture the signatures of subtle changes for successional forest cover while minimize the noisy effects that contaminate the multitemporal images.

Therefore, two research questions are asked, 1) How does LCLU change before and after the implementation of SLCP and NFPP around 2000? 2) What is the growth trend of GFG and natural forests since the implementation of the new policies? The hypotheses includes that the forest cover increases with less fragmentation and irregularity and both of

natural and GFG forest have positive growth trend of aggradation under the implementation of forest protection and restoration programs. To investigate these research questions, Tiantangzhai Township with natural reserve was selected as study area in southeastern Dabie Mountain of China. The overall objective is to track land cover and land use change before and after implementation of forest policies as well as to characterize the growth trend of both natural forest and GFG forest stands since 2002. More specifically, the research was conducted to: 1) map forest class within Tiantangzhai Township in 1992, 2002, and 2013 and analyze the forest landscape with/without GFG forest stands; 2) quantify the forest successional information by utilizing the Tasseled-Cap indices including brightness and greenness and track the temporal/spectral trajectories of all forest at whole region scale; 3) provide reference of GFG forest growing trend after SLCP implementation to policy makers for sustainable development of forest programs.

2. DATA AND METHODS

2.1 Study area

The Tiantangzhai Township, in Jinzhai County of Anhui province in China, is located in the eastern part of Dabieshan Mountain (Fig. 1). The township covers an area of 28,914 hectares (ha) with abundant forest biomass. The elevation of the area varies from 300 to 1700 m above sea level. The mild weather and sufficient rainfall, make it an optimal area for vegetation growth. Due to its remoteness, the region is characterized by low population and density. The transportation system is poorly-developed and thus brings inconvenience for the connections to big cities. Though the natural ecosystem is well preserved due to less intervention of human activities, the normal behavior such as animal hunting, forest harvesting by local residents still caused problems in environmental protection for decades before 21st century. On one hand, this region was established as the national reserve for forest conservation as one part of the entire NFPP in 1998. In response to the program, the environment was supposed to be protected from human interference, including forest harvest, wild life hunting. Almost every household owns land covered by natural forest and receives 8.75 RMB/mu each year (1 mu = 1/15 ha) from the central government. The government implemented SLCP in 2002 in Jinzhai County. Farmers receive an initial compensation of 230 yuan/mu/year for 8 years, and the renewed compensation of 125 yuan/mu/year for another 8 years. The total area of land planted with Grain-For-Green trees accounts for a

small proportion of the entire study area since only one sixth of all the households participated the forest restoration program.

2.2 Data acquisition and preprocessing

Three Landsat images were acquired in 1992, 2002 and 2013 from "USGS Global Visualization Viewer" (http://glovis.usgs.gov/). The availability of the imagery was mainly limited by the cloud coverage. One scene of WorldView-2 image with high spatial resolution was also requested. Detailed information of the satellite images were shown in Table 1. Though many algorithms have been proposed for the data without *in situ* atmospheric information, Song et al in 2001 suggested that there were limited improvements with more sophisticated approaches but a simple modified dark object method can have at least equally good performance for removing atmospheric effects. In order to characterize the spectral information with vegetation indices such as NDVI, all the Landsat images in this study were atmospherically corrected using simple dark object subtraction (DOS3) approach and the DN value was converted to the surface reflectance. The DOS method assumes 1% surface reflectance caused by the atmospheric conditions and the minimum DN value over one TM scene can be found at the value with at least 1000 pixels from the peak of the histogram for each band (Moran et al., 1992; Chavez, 1996). Digital Elevation Model (DEM) with 30 meter resolution was also obtained and projection including resampling was re-defined in order to match the Landsat images in terms of the spatial resolution as well as array alignment.

2.3 Classification and change detection

2.3.1 Random forest (RF) classifier

In recent years, many papers argued to use multiple classifiers to generate an ensemble classifier, which is believed to have higher accuracy for classifying remotely

sensed images than any with single classifier (Briem et al., 2002; Dietterich, 2002). A new and powerful statistical classifier proposed by Breiman in 1999 is called Random Forest (RF), which randomly chooses a set of features among all the included variables (e.g. spectral bands, topographic indices) to split each node within a single tree (classifier), and also generates a large number of such trees. The unknown pixel are assigned by voting it to most popular class from all the tree predictors. Breiman also stated that the generalization errors for forests always converge to a limit as the number of trees is very large. An increasing number of researchers employed this classifier in various fields because it generates high classification accuracy and has the capability of evaluating variable importance and of modeling complex interactions (Cutler and Stevens, 2006; Archer and Kimes, 2008). Pal (2005) compare two machine learning classifiers with Landsat Enhanced Thematic Mapper Plus (ETM+) data and he argued that the random forest classifier has equal performance in classification accuracy and training time but requires fewer user-defined parameters. Prasad et al (2006) also tested four statistical algorithms of vegetation mapping and found the Random Forest was superior in predicting current distribution of tree species. In this study, random forest classifier was used through all the processes of classification.

2.3.2 Automatic Adaptive Signature Generalization (AASG)

To keep the consistency of classifications for remotely sensed images with time series, Automatic Adaptive Signature Generalization (AASG) proposed by Gray and Song (2013) was employed to adapt spectral signatures of each of the individual Landsat imagery. This method identifies training data from features that are stable throughout time. It requires the high accuracy of the most recent image classification to be as the reference image for which the reliability of training data can be examined. The assumption made for this

approach is that the majority of the pixels did not change if the image is for a sufficiently large area. By subtracting image bands of two different time period, the stable sites within reliable range can be located around the mode of the histogram of the difference image. These stable pixels are further filtered and selected as training data to classify their corresponding image (Fig. 2). Previous study indicated that the AASG is flexible with respect to any supervised classification algorithm and showed a better performance for irregular time series comparing with traditional signature extension.

2.3.3 Classification of Landsat images

In this research, random forest (RF) was selected as the classifier for both the reference map and the AASG approach. Considering the prevalence of vegetation over the mountainous area of this study site, spectral and topographic derivatives were generated from remote sensing images as well as ancillary data in order to increase the separability of the classes. A set of vegetation indices were calculated from the atmospherically corrected images including simple ratio (Jordan, 1969), normalized difference vegetation index (Rouse et al., 1973), structural index (Fiorella and Ripple, 1993a), modified normalized difference water index (McFeeters, 1996; Xu, 2006), enhanced vegetation index (Huete et al., 1997). Several topographic indices were also derived from digital elevation model (DEM) dataset including: elevation, slope, aspect, topographic wetness index (Beven and Kirkby, 1979).

To create the reference map of 2013/5/21 Landsat image, the RF classifier was trained with user defined pixels by referring to the high spatial resolution image WorldView-2 (2013/7/13). The training sites for the WV2 image were collected in the field with the assistance of GPS during summer 2013. Twenty percentage of the pixel values as training points were randomly picked and reserved for the accuracy assessment of the classification

for the reference map. Based on the experience and local knowledge of the land use within study sites, nine land cover types were defined: build-ups, deciduous forest, coniferous forest mixed forest, water, cropland, rock outcrop, and barren area, and shrub/grass.

In generating the classified maps for target images (Landsat image of 1992/10/18 and 2002/10/6), the AASG method was modified and improved based on Gray and Song (2013). Firstly, the NDVI band calculated from red band and near infrared band was chosen for image differencing instead of merely using red band or near infrared band. Because the study area was dominated by vegetation, including both the near infrared band and the red band therefore contains more information associated with the stable sites. Second, multiple c parameter for each class was defined instead of using global c parameter which defines the thresholds of selecting stable sites. In Gray and Song (2013), the global c parameter of 1, 0.5 and 0.25 were selected to test the threshold sensitivity which may cause the overabundance problem of stable sites for a particular class such as vegetation. So the c parameter was set by restricting the number of stable pixels to 1000 with each class in this study. If the total number of stable pixels is less than 1000, then the interval would be limited to match the number all pixels for such stable sites of the class (Fig. 3). Third, since AASG is flexible for any classifier, the random forest was again used in this approach and also was trained by the extraction of the spectral information, vegetation indices and topographic properties of those pixels selected as training sites.

2.3.4 Classifying WorldView-2 image and "Grain-for-Green" forest stands delineation

Due to the high spatial resolution of the WorldView-2 image, the classified map as foreseen can be filled with "speckle" noise particularly for those with high spectral variations and those at the boundary of different classes. So more specific categories were defined for

some classes such as build-up areas, agricultural land. The specific categories within one general group were then combined as one class. The general classes were: build-up area (open, pitch, residents), water (river, pond), forest (deciduous, coniferous, mixed), farmland (cropland, dry land), barren land (rock, open). The clouds associated with their shadows were removed from the entire scene. A 5 by 5moving window majority filtering was carried out to reduce the speckles.

It is challenging to identify the "Grain-for-Green" (GFG) forests merely based on the satellite image itself because of the confusion with natural forests in terms of the spectral information. Additional data were acquired including topographic map depicting each GFG forest stands associated with the ID, location and area, and the data that monitored the progress of GFG forest by households in 2009. The technician in the local township forest station also provided personal experience on locate each GFG patch on the WorldView-2 image. 226 GFG forest stands were depicted in ArcGIS and exported as a vector layer of GFG forest class. Fortunately, all the forest stands are free of the cloud cover. The vector layer were then stacked to the Landsat images for further analysis of forest growth trend.

2.4 Landscape Pattern Metrics

During the past decades, numerous landscape pattern metrics have been proposed for analyzing the composition and configuration of landscape structure and spatial patterns as well as their application in relationship with the sustainability for land planning (Turner and Gardner, 1991; Ribeiro and Lovett, 2009; Su et al., 2011). The changes in landscape structure triggered by the land use/cover change has strong influences on the changes of ecosystem functions and vice versa (Leitão and Ahern, 2002). The landscape process measurements of the extent to which the patches are fragmented or aggregated can be of importance to monitor

the change of biodiversity. In this study, a set of class-level metrics based on the research questions were selected including total area (TA), patch density (PD), edge density (ED), mean patch area (MPA), mean perimeter area ration (MPAR). The calculated metrics were then used to compare the landscape patterns between natural forest without GFG forest stands and all the forest including GFG forests. It was also applied to the each forest class including deciduous, coniferous and mixed forest.

2.5 Growth trend of successional forest covers

The growth trend of the GFG forests stands pertains to the monitoring of forest successional change which has implications for land use management as a fundamental ecological process (Song et al., 2002). In this research, the temporal trajectories of the GFG forests were examined in the brightness and green space (B-G space). The pixels of forests were generally spread along a line in the B-G space, which is regarded as canopy closure line (CCL) in this study. Once the canopy were closed, the forests at early stages located at the higher end of CCL with both high brightness and greenness values. As forest succession continues, increased mutual shadowing in the canopy leads to the decrease of both brightness and greenness. As a result, forests move towards the lower end of CCL as they mature. In order for the multitemporal image data to be comparable, both brightness and greenness were normalized to Z-score values separately.

The CCL was defined as a parallel segment of the linear regression line of points at left side of the tasseled cap. Given small ranges of greenness, the points with the lowest brightness within each range were filtered as candidate points on the canopy closure line. A trend line is then fitted to these candidate points to identify the CCL. The upper bound and

lower bound of the segment are limited by the maximum and minimum vertical points of the pixels respectively (Fig. 4).

The successional information of forests was considered as a combination of two indices: closure index (CI) and maturity index (MI). The closure index is related to the perpendicular distance of a given point to the canopy closure line and is estimated as:

$$CI = \frac{(d_{max} - d_i)}{d_{max}} \quad (1)$$

Where d_{max} is the distance of the pixel which has the largest distance to the CCL, d_i is the distance of the i^{th} pixel to the CCL. The larger the value is, the more the pixel is likely to be forest with closed canopy. The other index represent which group of successional stage the forest belong to and is estimated as:

$$MI = \frac{L_{i,upper}}{L} \quad (2)$$

Where $L_{i,upper}$ is the length of segment at CCL between vertical point of a given pixel and the upper bound along CCL, and L is the length of CCL between upper bound and lower bound. The CI and MI each have limitation to represent the successional information, so a synergistic successional index called SynI was developed as the product of these two indices:

$$SynI = \frac{(d_{max} - d_i)}{d_{max}} \times \frac{L_{i,upper}}{L} \quad (3)$$

The index values of CI, MI, and SynI all ranges from 0 to 1. The SynI represents a combined information of both canopy closure and successions. The larger value denotes that the forest pixel is closer to old-growth forests and lower to the young forests.

Regressions with vegetation indices proposed by previous studies was conducted for each year to evaluate the actual meanings of these indices generated. Then the GFG forest stands were partitioned into 3 levels by the difference of SynI between 2002 and 2013 in

order to monitor the growing trend of these planted trees. The topographic and vegetation indices for each level were extracted to validate the effects of the difference at levels.

3. RESULTS

3.1 Land cover and land use change detection

The classified maps of the three Landsat images are shown in Fig. 5. The 2013 classification as reference image has overall 92% accuracy with Kappa coefficient over 0.9. The classifications in Year 1992 and 2002 were generated using AASG methods. The change detection statistics for forest, cropland and shrub/grass land were summarized in Table 2. From 1992 to 2002, the overall forest area does not change much while there is 13.96% increase from 2002 to 2013. Before the implementation of forest conservation and restoration programs, the areas of deciduous and coniferous forests declined while that of mixed forests increased. However, during the decade after the program, deciduous and mixed forests both have substantial increases in study area. The tree species provided by the government for the program were mainly deciduous forests which have relatively higher survival rates.

The cropland had limited increase before the SLCP implementation and declined by 11.12% partially because of the conversion from participated farmland to the GFG forests. It is also notable that there is great amount of decrease for shrub/grass land (-61.29%). The shrub and grass land have the largest confusions over all the classification particularly at the boundary between forest cover and non-forest vegetation land cover. The major transformation has occurred from the shrub/grass land to the deciduous and mixed forests. The natural forests and the young trees planted by local residents have gradually become the dominant land cover over the other vegetation types and thus led to the substantial change.

3.2 Synoptic forest landscape pattern change

The class-level analysis of landscape metrics offers a general landscape pattern of forest including GFG stands and excluding GFG stands (Fig. 6). The interpretations for each metric were summarized in Table 3. Since the total area of GFG forest stands is relatively small compared with the natural forests within the township, the landscape characteristics generally have little changes for the forest covers with and without GFG forests. Though the decrease of total area for forest without GFG forest is negligible, such slight changes can be observed via other metrics that all the forest cover with GFG forests were less fragmented at class level with 2.6% higher of patch density and 1.1% higher of edge density if the GFG forest were clipped out. The lower, not substantial though, mean patch area (MPA) and mean ratio of perimeter to area (MPAR) of forests indicated the irregularity and complexity of the forest patches without GFG forests.

3.3 Spectral/temporal trajectories of all forests

3.3.1 Spatial and temporal pattern of all classes

The scatter plot of transformed "tasseled cap" of Landsat 8 OLI image of 2013 is shown in Fig. 7. It should be noted that the data points are so dense that the majority of them were overlapped, particularly for deciduous, coniferous and mixed forests. So the mean values of normalized brightness and greenness of each class are also plotted to clearly display the spectral distribution in brightness-greenness (B-G) space of Tasseled Cap transformation. The classes of barren land and open rock, accounting for a tiny portion of the entire study area, were excluded in the figures. The relative patterns of each class indicates that forests are compactly spread along a line on the upper left side of the "tasseled cap" with higher greenness than the other classes in general. For the closed canopy forest classes, the

measured surface reflectance is mainly from the vegetation with limited contribution from the background. Along this canopy closure line, it is believed that both greenness and brightness decrease as the forest grows because of mutual shading as the trees getting bigger. The deciduous forest, colored in light green in Fig. 7 has higher values of both brightness and greenness due to higher reflectance from broad leaf species. The coniferous forest, colored in dark green in Fig. 7, appears to have lower values in both brightness and greenness due to its relatively lower reflectance compared with the broad leaf species. Mixed forest accounting for the majority of forest pixels is located between deciduous and coniferous forest with wider spread due to its higher variety in terms of spectral signature. The shrub/grass land also have relative higher brightness and greenness but below the forest at canopy closure line. This is reasonable due to the sunlit background in addition to their high reflectance at green wavelength. The cropland, however, is located below the forest and shrub/grass cover with points widely spread due to the properties of various crops planted. There is variety of crops during the time of image acquisition, ranging from the higher brightness for open land after the crop harvest, and other crops at varying stage of development. The water class has the lowest surface reflectance, and thus is neither bright nor green. The complexity of the build-up class make it possible that the points widely spread in the B-G space but generally have high brightness and low greenness due to the spectral properties associated with concrete, pitch, cement in the residential areas. Similar spectral patterns of Tasseled Cap transformation were also observed for Landsat 5 TM image in 1992 and Landsat 7 ETM+ image in 2002.

The stable pixels of forest, cropland and shrub/grass class in all three years were filtered for examining the temporal trajectories in B-G space (Fig. 8). The mixed forest, as

the dominating class in the study area, is the most stable class of spectral signature through the two decades. The temporal trajectories of mixed/deciduous forests are different from that of coniferous forest. During the two decades, mixed and deciduous forests are basically stable with little changes for both brightness and greenness. While coniferous forest keeps moving to the old-growth during the two decades. This can be attributed to the occupation of young pioneer trees at early stage on the shrub/grass land triggered by the implementation of forest conservation and restoration programs. The amount of the conversion from shrub/grass to deciduous forest is relatively large and it thus leads to the movement of such forest spectral signals towards early successional stages with increase of both brightness and greenness. The large change of the cropland between 1992 and 2013 may due to multiple reasons such as the activities of cultivation by local farmers as well as phenological responses of crops to the seasonal weather changes. Despite the temporal change of stable classes, the general spatial pattern maintains that there are no overlap among temporal trajectories of any two classes in terms of the mean values.

3.3.2 Spectral/temporal trajectories with successional indices

Fig. 9 provides an illustration of depicting canopy closure line (CCL) in B-G space of 2013 Landsat 8 OLI image. Assuming a reasonable accuracy of classification, the pixels of forest are located closer to CCL than those of other classes. So only points classified as forests were plotted to define the canopy closure line, which is assumed to be above all the points of the study area. In the case of 2013 image, the greenness value of the pixel with minimum brightness is 2.6215 and the maximum greenness value is 2.9024. Small steps of 0.01 for greenness from 2.63 to 2.91 was set to identify all the points required on defining CCL within the range. The point with the lowest brightness in each step was selected. After

the points from all steps were identified, we can fit a regression line as the CCL. Keeping the slope (0.7518) fixed, the trend line was shifted until all the points were at or below it, which leads to an intercept of 0.9010 for the 2013 Landsat 8 OLI image. The line was then segmented with regard to upper and lower bound based on the pixels. The parameters for defining successional indices for all the three years were listed in Table 4. The upper bound of brightness and greenness and length of the CCL were used for calculating maturity index.

The temporal changes of mean distance to CCL and the $L_{i,upper}$ of CCL for all forests and each forest category were examined in Fig. 10. It is not surprising that there is consistency between these two quantitative measures and the visual observation in temporal trajectory of each class. From 1992 to 2002, the mean value of distance to CCL for all categories has modest increase and a significant decline during the next decade, indicating increase of canopy closure since 2002. As for the $L_{i,upper}$ of CCL for a given pixel in the B-G space, the mean values for all categories except coniferous forest have increased during the first decade and moderately declined during the following decade. For similar reasons, this may also be attributed to the conversion from non-forest vegetation to the young forests, most of which belong to the deciduous forest or contribute to the mixed forest.

Different from the distance to the CCL and the $L_{i,upper}$ of CCL, the SynI index was developed as a relative measure over all the forest pixels given one point within the study area. Therefore the temporal change of the d_i and $L_{i,upper}$ can be different from this index that the latter more accurate in measuring the successional stage of a pixel relative over the entire forested pixels (Fig. 11). It can be observed that the closure index has decreased from 1992 to 2002 and increased rapidly since the forest programs, which indicates the changes in terms of forest canopy structure as trees established for the recent decade. The values and change

patterns of mean closure index are similar for all the four categories. For maturity index, however, the temporal trends are different, particularly for coniferous forest. Though the overall values decreased from 2002 to 2013, the relatively higher magnitude of CCL length increase over that of distance to CCL upper bound leads to slight decline of maturity index. Vertically, coniferous forest has highest value and deciduous has the lowest, which agrees with the results that deciduous forests are at early successional stage while coniferous forest is mainly at old-growth stage. The product of these two indices (SynI) were calculated to the track the temporal change of the forest at different successional stages. Seen from Fig. 11, the SynI values follow the patterns of maturity index across forest classes because of the higher magnitude of maturity index. However, the temporal changes are slightly different from CI and MI. In general, the deciduous forest at bottom did not change significantly during the two decades while the index values for coniferous and mixed forests have increased after the implementation of programs. The aggradation of coniferous and mixed forests may result from the conservation of the natural forests that trees in remote area were protected from logging by local residents. The stable change of deciduous forest may due to both the restoration of GFG forest stands and conversions from other land covers. The plant of trees contributed to the increase of closure index while the transformation of land covers caused the decline of maturity index.

The scatter plot shows the successional synergistic index of all the forest pixels in 1992, 2002 and 2013 (Fig. 12). The overall distributions of index levels are similar that higher values of SynI are located at the lower left corner in the brightness and greenness space. As the brightness and greenness increase, the SynI value decreases to 0 closer to the upper end of CCL where a recently closed canopy stand locates. The pixels in 1992 and 2002

are spread more widely than those in 2013 when the pixels are packed more closely towrds the CCL. This is because there are more pixels having lower SynI values resulting from the lower values of MI for the first two years. The changes of observed spectral trajectories in 1992 and 2002 in terms of the spread of high SynI values. In 2013, the highest value representing the old-growth forest is close to 1 with the indication of late succssions of these forest pixels which were actully classified as coniferous forest. This distinct phenomenon in 2013 is probably a result from the forest protection and restoration programs. The majority of the pixels in forest area with initial low SynI tend to move faster to the CCL in response to the natural growth in mountainous environment. Actually, there are larger amount of pixels with higher CI values (not shown in the figure) in 2013 indicating the increase of number of stand with closed canopy, thought the MI values don not change much. Besides, the proportion of very low CI values for all forest in 2013 is smaller than those in 2002 also confirms forest aggradation in the recent decade.

The scatter plots of SynI for deciduous, coniferous and mixed forests in 2013 were displayed in Fig. 12. It is observable that the deciduous forest dominate those at early successional stage with very low SynI values while coniferous forest has more pixels with high values than the other two categories except for a small group of pixels. This is probably because of the misclassification in land cover mapping due to topographic shadow effects. Within the mountainous region, the deciduous forest at the shading aspect have much lower reflectance of solar radiation and may appear dark green resembling that of coniferous forest. After Tasseled Cap transformation and normalization of brightness/greenness, this group of pixel considering as coniferous forest may actully be deciduous or mixed forest in reality.

3.4 Growth trend of GFG forest stands based on successional index

3.4.1 Temporal trajectories of GFG forest stands

Based on the topographic map with GFG forest locations marked as a polygon, GFG stands were manually delineated on the WorldView-2 image. There are a total of 226 GFG stands in total for the Tiantangzhai Township. The polygons was then overlaid on Landsat images to extract the brightness and greenness values for these polygons. All the stands approved by local forest station are included regardless of the actual ground conditions. Therefore, a group of pixels labeling as GFG forest stands may be classified as non-forest in the Landsat classification and thus may not be properly measured by the forest successional indices developed earlier in this study. The temporal trajectory of the average GFG forest in normalized B-G space was shown in Fig. 13. From 1992 to 2002, the overall brightness of land to be GFG forest is stable with little change while the increase of greenness is observed. This if primarily caused by the conversion of planted crops to grass cover. Before 2002, these GFG forest stands should be recognized as croplands. The participated patches of lands were considered by local farmers as to be poorly productive. The trajectory, after 2002, has changed its direction towards less bright and green as GFG forest established. This can be explained as the result of successional forest creating shadows within the forest stands.

The termporal changes of distance to CCL and $L_{i,upper}$ as well as the forest development indices were plotted in Fig. 14. The SynI values for GFG forest stands are less than 0.2 in 1992 and 2002 but increase to 0.24 in 2013. Meanwhile, the extent to which the CI increase (greater than 0.5) also has taken place in the recent 10 years. During the first decade, there was not much change because these indices were meaningful for pixels defined as forests. However, it is possible to track the growth trend by comparing the change during

decade before and after the implementation of forest programs. As stands were established in 2002, the conversion from croplands to froests have stronger influence to CI derived from the distance to CCL. Such critical change is reasonable because of the replacement of tree canopy over the backgound. The MI does not change during the two decades though there is slight increase of $L_{i,upper}$ from 2002 to 2013. This follows that the planted trees caused the movement of pixels to lower brightness and greenness along CCL, but contibuted to more young forest relative to the natural forests around. The incease of the SynI after forest restoration program demonstrates the overall aggradation of the GFG stands which is mainly from the large magnitude of increase in CI.

Fig. 15 shows the scatter plots for each group of pixels labeled as GFG forest stands through the two decades. The pixels with negative mean values were filtered out, meaning the distance on average to the CCL was even larger than the maximum for natural forests. These forest stands were regarded as trees that have not met the criteria of well growth until 2013. In this part, 15, 20 and 3 GFG forest stands were excluded from the scatter plot of 1992, 2002 and 2013 respectivly. On one hand, the points for 1992 and 2002 spread wider in the normalized B-G space and the majority of them have low values (less than 0.5) in terms of the succession SynI; on the other hand, those GFG forest stands in 2013 are more compact and the highest SynI value is over 0.54 colored in light green at lower left of the B-G space. It can be found that the distribution as well as the SynI value are able to characterize the change for the GFG stands since the implementation of forest plocies, particularly the restoration program. The overall tendancy of the pixels within GFG forest stand is closer towards the CCL in 2013. Furthermore, the highest SynI values with both low brightness and greenness are probably due to the agradative development after establishment.

3.4.2 Correlations between CI, MI, SynI and vegetation index

To examine the implications of the developed forest indices, regression analysis was employed to find the correlations between these indices for GFG forest stands and vegetation indices in previous studies. The illustration of the regression results of forest successional indices and strucutral index (SI, badn ratio of TM 4/5) in 2013 were shown in Fig. 16 (other correlations not shown).Among all the possible vegetation indices, the structural index (TM 4/5 ratio) proposed by Fiorella and Ripple (1993) were found to be positively correlated to CI and SynI for all the three years (R^2>0.7), but the relationship is weak for maturity index(R^2=0.16). Such high correlation is believed to result from the strong relationship between forest canopy and structural characteristics. As stand age class falling into 0-10, the growing leaves can be determining factors that influence the characteristics of canopy structure which at the same time promote the canopy closure. Previous studies (Running et al., 1989) also mentioned that the structural index can not distinguished old-growth forest with young forest before the canopy closure which explains the poor connection of MI and SI values. For 2013, interestingly, saturation problem of structural index occurs as the SynI increases in the regression with relatively low R^2 (0.31) comparing with that for CI. This numerically is because of inverse change ,limited though, of SI with change of MI. Also notice that the variation SI is getting larger as MI increase. This provides the evidence of insensitivity of structural index to the extent of forest maturity with age regarding the successional stages. After the saturated point in SynI-SI regression of 2013, the SynI has better capapbility of tacking the successional information on both maturity and canopy closure that SI yet reaches the highest values and keeps unchangeable. In fact, MI values are highly correlated with enhanced vegetaion index (EVI) for all the three years (R^2>0.6). The

EVI was developed by adding spectral information from blue band to red and near infrared bands of Landsat image in order to minimize the effects of background and atmophere (Jiang et al., 2008). This vegetation index is senitive in monitoring tree growth particularly with abundant biomass and hence less prone to be saturated which also is applied to the MI proposed in this study. As for the normalized difference vegetation index (NDVI), the correlations with CI or MI are roughly around 0.5 but much weaker for SynI with strong saturation problem of NDVI values.

3.4.3 Growth trend of GFG forest stands

Regarding the potential of forest indices for measuring forest successional information, the difference of SynI between 2002 and 2013 was taken as an indicator for estimating the growth trend of GFG forest stands. Among all the forest stands, 3 levels of the extent to which the trees have been growing were developed: poor-developed, moderately developed and well-developed. Considering the mountainous area of this natural reserve, the topographic effects should be taken into consideration for examination. The topographic information and vegetation indices were then extracted for each level to evaluate the effects on the growing trees at early stages. Fig. 17 a), b) and c) show the distributions of elevation, slope and aspect of GFG forest stands with different levels. The well-developed GFG forests are mainly located in area with lower elevation and flatter slopes, with which the natural environment may be suitable for the natural growth of trees planted. Furthermore, it is more likely that such topographic conditions allow easier access for household to manage the forests particularly during the first few years. For the well-developed forest stands, the largest proportion lies around aspect facing southwest while that for poor-developed were facing east. The moderately-developed forest stands has pretty even distribution across all the

direction. The temperature over the whole study area has little fluctuation through decades plus sufficient precipitation, the sunlight therefore can be the primary limitation for GFG forest growth. The southwestern solar radiation received by trees provides with abundant energy for photosynthesis meanwhile minimized the shadow fraction caused by canopy of surrounding forests. Moreover, the fraction of shadowed canopy by GFG forest themselves can also lead to the change of brightness/greenness and thus the forest indices developed.

Fig. 18 shows the vegetation index changes of the 3 development levels of GFG forest based on the SynI difference. The plots consolidates the growth trend of aggradation for the trees planted since 2002. All the vegetation index values are positive with indication of the general aggradation of GFG forests. Larger differences of the calculated vegetation indices are observed for well-developed forest stands comparing with moderately-/poor-developed stands. As a result, the growth trend of the 3 levels can be well-detected using the measurement of successional forest index in terms of the evaluation by the vegetation indices.

4. DISCUSSION

4.1 Classifications and landscape analysis

This study tracked the land use land cover changes in Tiantangzhai Township under the implementation of forest policies at the beginning of 21st century. The classification for change detection and landscape pattern characterization emphasized the natural forest and GFG forest stands in response to natural forest protection and Grain-for-green forest restoration respectively. In this case, the machine learning method called random forest (RF) as the classifier was employed and modified automatic adaptive signature generalization (AASG) as the approach extracting image-based training sites was used for all the process with remotely sensed data. As pointed out by Gray and Song in 2013, the error sources of AASG were mainly from the misclassification of reference image and the filtering of stable pixels with multitemporal imageries. The high quality of classifying the reference map (2013 Landsat OLI image) was satisfied by referring to the fine spatial resolution image from WV-2 satellite as well as the GPS points collected in field work during summer 2013. The overall accuracy over 90% of the initial reference map ensured the minimization of the accumulated errors for further classifications. The modifications of AASG approach include adding bands of vegetation indices and Tasseled Cap indices, which make it necessary for absolute atmospheric correction in converting DN values to reflectance scaled from 0 to 1. Because Landsat OLI product was released in 16-bit radiometric resolution, ridge method was also applied as relative atmospheric correction to match TM and ETM+ image reflectance to that

of the most recent one in response to the sensor difference. This also leads to the process of normalizing brightness and greenness indices separately after Tasseled Cap transformation.

Although the 2013 reference map was generated with high accuracy especially for the natural forest, there may still exist substantial amount of misclassified pixels for each specific forest category when applying automatic stable sites due to multiple factors. The change detection statistics revealed a large difference of conversion among deciduous, coniferous and mixed forest, on which the phenological change may have strong effects. The dates acquiring 2013 OLI remotely sensed data is May 21 in early summer but the previous images (1992 and 2002) were captured by satellites during October. The seasonal change of vegetation, though not as critical as cropland, accounts for a certain amount of the land cover change areas over natural forests and shrub/grass land classified. The sun angels across the seasons should also be taken into consideration. The sun light with higher elevation angle in during May could have more penetration to the forest canopy which further causes less reflected signals received by the sensor. Besides, the topographic effects is another error sources influencing the brightness reflected by trees at sloping facing different directions. One of the limitations of AASG approach lies in the selection of stable pixels based on band subtraction that contains nothing but reflectance information. Future improvements may consider the inclusion of topographic effects for training samples filtering in addition to the classifier.

The landscape pattern change with conversions of pieces of land to GFG forest is not significant mainly because of three reasons. Firstly, almost every household own the natural forest protected from logging but only about a sixth of them participated in Grain-For-Green programs. The relatively small proportion of the GFG forest stands in terms of total area has

much less contribution to substantial change of class-level metrics at the entire landscape of study region. Though the general pattern indicate less fragmentation of forest as GFG forest established, the metric analysis at patch-level may be more sensitive to young growing trees over the large scale. Second, the GFG forest identification was referenced on the data from topographic map decade ago. The accuracy of location and area for each GFG forest stand basically depends on the personal experiences by local farmer and staff from forest stations. Since the establishment of trees, it is further hard to monitor the growing trend of each forest stand particularly for those at remote region with limited access. Thirdly, the forest at early successional stage can leads to confusions with natural forest and other class such as abundant shrub/grass due to their weak contribution in terms of reflectance observed from satellite images. As a result, it is inevitable that some stands labeled as GFG forest have actually been poorly-developed and thus classified as non-forest cover. These factors overall undermined the positive impacts of the planted young trees to the natural forest as a whole.

4.2 Temporal trajectories of natural forest

Considering the limitations of classification in forests at different successional stages, this study proposed the development of forest indices extracting mature and canopy closure information from the brightness/greenness space after Tasseled Cap transformation. It is required to generate high quality classification maps because the distribution of the each class is crucial for calculating the forest indices. This was examined by the spatial/temporal characterizations of pixels with each class in the normalized brightness/greenness space. The assumption lies in the relative positions of each category particularly forests when defining the upper/lower bounds along the canopy closure line as well as the maximum distance to the line. Noting the variety of shape of tasseled cap transformed from images of each year, the

absolute value of the length of CCL and distance to CCL are in fact incomparable among multitemporal data. Multiple factors can result in this discrepancy in forming Tasseled Cap. One of the reasons includes the environmental stress on the forests over the entire Tiantangzhai Township. According to the sensitivity of vegetation area to the precipitation, for example, the overall greenness may shifted down in response to drier conditions. Besides, sensor difference also occur even the coded DN value was converted back to the surface reflectance and such transforming process of reflecting signals would inevitably cause information loss and thus influence the distributions of pixels in B-G space.

Therefore the relative location of given pixel over all the points spreading in B-G space was considered within tasseled cap which also normalizes the value to the range of 0-1. In this research, CI and MI are relevant to the maximum distance to CCL and length of CCL respectively with restriction to the pixels classified as forest cover. It is possible to generalize the restriction to the points within the whole study area. For example, noticing the distribution of build-up with much higher brightness and lower greenness than other class, its mean value of B-G coordinates can be a candidate for determining the maximum distance to CCL. As for the MI based on CCL length, forest pixels seems to be adequate in defining the upper and lower bound.

Due to the fact that the forest indices are derived from the tasseled cap indices of forest cover, the actual meaning is confined to the quatification of forest successional information. Though band math is plausible for creating the index bands, the pixels over the defined “maximum” distance to CCL would have negative values meaning nothing further from unlikely forest. This also happened when the pixel lies outside the CCL bounds. Seen from the scatter plot of each class in B-G space, it is undoubted that the majority of pixels

classified as build-ups, cropland and water would have negative index values. At this point, the sensitivity of the defining maximum distance and bounds along CCL was suggested for further analysis. The selection of study area should also be taken into account with certain size dominated by forest.

4.3 Growth trend of GFG forest stands

A certain amount of pixels labeled within GFG forest stands have negative value of SynI for all the three years. It is reasonable for the images in 1992 and 2002 since those patches depicted were actually cropland or abandoned land belonging to non-forest cover. However, negative values also exist for the image in 2013. Except for the errors from misinterpretations, it is likely that the ground truth of these pixels within GFG forest stands are non-forest due to the growing failure of trees since established in 2002. These pixel with negative value, as a result, are regarded as the non-forest and removed from the scatter plot with z-valued ranged 0-1. However, all the pixels were included for calculating the mean indices to measure the extent of stand aggradation or degradation. The purpose is to track the growth trend of each forest stand during the decade of forest policy implementation which manifests the advantages of remotely sensed data in monitoring forest at early successional stage over the in situ management. Fig. 19 provides the illustrations of forest stands at different levels on WorldView-2 image in 2013. It can be observed that the well-developed forest (a) stand has more homogeneous canopy cover while the area of grass/shrub background is outstanding within the poorly-developed stand (c). It is more likely to cause negative SynI value when there is large open area of background with higher brightness. For the moderately-developed stand (b), the canopy closure status undermine the CI value despite the higher MI for the trees in dark green.

5. CONCLUSIONS

Since 2002, substantial land cover changes have taken place following the implementations of forest conservation and restoration programs in Tiantangzhai Township until 2013 compared with the changes during the decade from 1992 to 2002. Overall natural forests prevail the study area with an increase of 14 percent. Large amount of shrub/grass lands have been converted to other land covers. The decline of cropland was also observed after the Grain-For-Green program. Though subtle, landscape metric analysis revealed that the forest landscape became the less fragmented and isolated for all the forest as well as each forest category (deciduous, coniferous and mixed) when the GFG forest stands were included. Such subtle changes require accurate spectral signals to characterize change associated with forest succession.

The development of forest succession were examined in the brightness/greenness space of the Tasseled Cap transformation. The distribution of pixels classified as forest in the brightness/greenness (B-G) space makes it possible to characterize the forest at different successional stages. In this study, 3 indices for forest development were developed in the brightness/greenness space. The closure index (CI) is relevant to the distance of given pixel to the canopy closure line which is defined as the regression line along the left edge of the tasseled cap. This index can be used as an indicator of the canopy structure as it has strong correlation with structural index (SI). The maturity index (MI) pertains to the stage to which

the stand is growing. Along the CCL, the pixels of young forest mainly lie at the top of tasseled cap with higher brightness and greenness. As the forest develops, the brightness and greenness value decrease. The synergistic successional index (SynI) was calculated as the product of CI and MI in order to combine the information from both. Regressions of the forest indices with vegetation indices indicates that SynI is highly correlated with SI, but more sensitive to young forests that has not reached canopy closure. In 2013, the pixels of all forests are packed more closely to the CCL in normalized B-G space indicating forests are generally in aggradation which can also be characterized by the increase of SynI values.

The temporal trajectory of GFG forest stands showed the spectral signals of changing brightness and greenness through 20 years. From 1992 to 2002, there is substantial increase of greenness with stable brightness which is due to the establishment of tress on pieces of land. During the following decade, both brightness and greenness declined as the young forests grew. The planted young trees impacted the change of CI, leading to the increase of SynI. The overall aggradation for GFG forest stands was also observed. Based on the extent to which SynI increase, the GFG forest stands were divided in to 3 levels poorly-developed, moderately-developed and well-developed. The topographic effects were observed within different levels that the stands with positive growing trend are more likely to appear at lower elevation and gentler slopes facing southeast with sufficient solar radiation. The growth trend with different level was also examined by the measures of vegetation indices. For validation of these indices proposed, *in situ* data were required measuring the actual reflectance of each forest category and testing the sensitivity of the defining the distance to CCL as well as length of CCL should be emphasized.

TABLES

Table 1. Landsat imagery acquired for the year of 1992, 2002 and 2013 (Path/Row: 122/38)

Year	Date	Satellite	Sensor	Multispectral resolution	Panchromatic resolution
1992	October 18	Landsat 5	TM	30 m	15 m
2002	October 6	Landsat 7	ETM+	30 m	15 m
2013	May 21	Landsat 8	OLI	30 m	15 m
2013	July 13	WorldView-2	-	2 m	0.5 m

Table 2. Statistics of change detection for forest, shrub/grass land and cropland

Class	**1992-2002 (%)**	**2002-2013 (%)**
Overall forest	-2.83	13.96
Deciduous forest	-8.07	18.80
Coniferous forest	-32.35	-73.40
Mixed forest	18.42	43.29
Cropland	3.06	-11.12
Shrub/Grass	12.17	-61.29

Table 3. Interpretation of landscape metrics selected.

Metrics	Interpretation
Total area (TA)	the sum of the areas (m2) of all patches of the corresponding patch type
Patch density (PD)	the numbers of patches of the corresponding patch type divided by total landscape area (m2)
Edge density (ED)	edge length on a per unit area basis that facilitates comparison among landscapes of varying size
Mean patch area (MPA)	average area of patches
Mean perimeter area ration (MPAR)	the mean of the ratio patch perimeter. The perimeter-area ratio is equal to the ratio of the patch perimeter (m) to area (m2)

Table 4. Parameters for calculating forest successional indices.

Parameter	1992	2002	2013
k	1.0868	1.1511	0.7518
m	2.1428	2.3241	0.9010
d_{max}	3.3216	2.8962	1.9512
L	7.0614	8.9111	9.7444
B_{upper}	1.3175	1.8755	3.1682
G_{upper}	3.5746	4.4830	3.2828

In the table, k and m denote the slope and interception of CCL. d_{max} is the maximum distance of the all forest pixels to CCL. L is the length of CCL. B_{upper} and G_{upper} are the coordinate of upper bound of CCL.

FIGURES

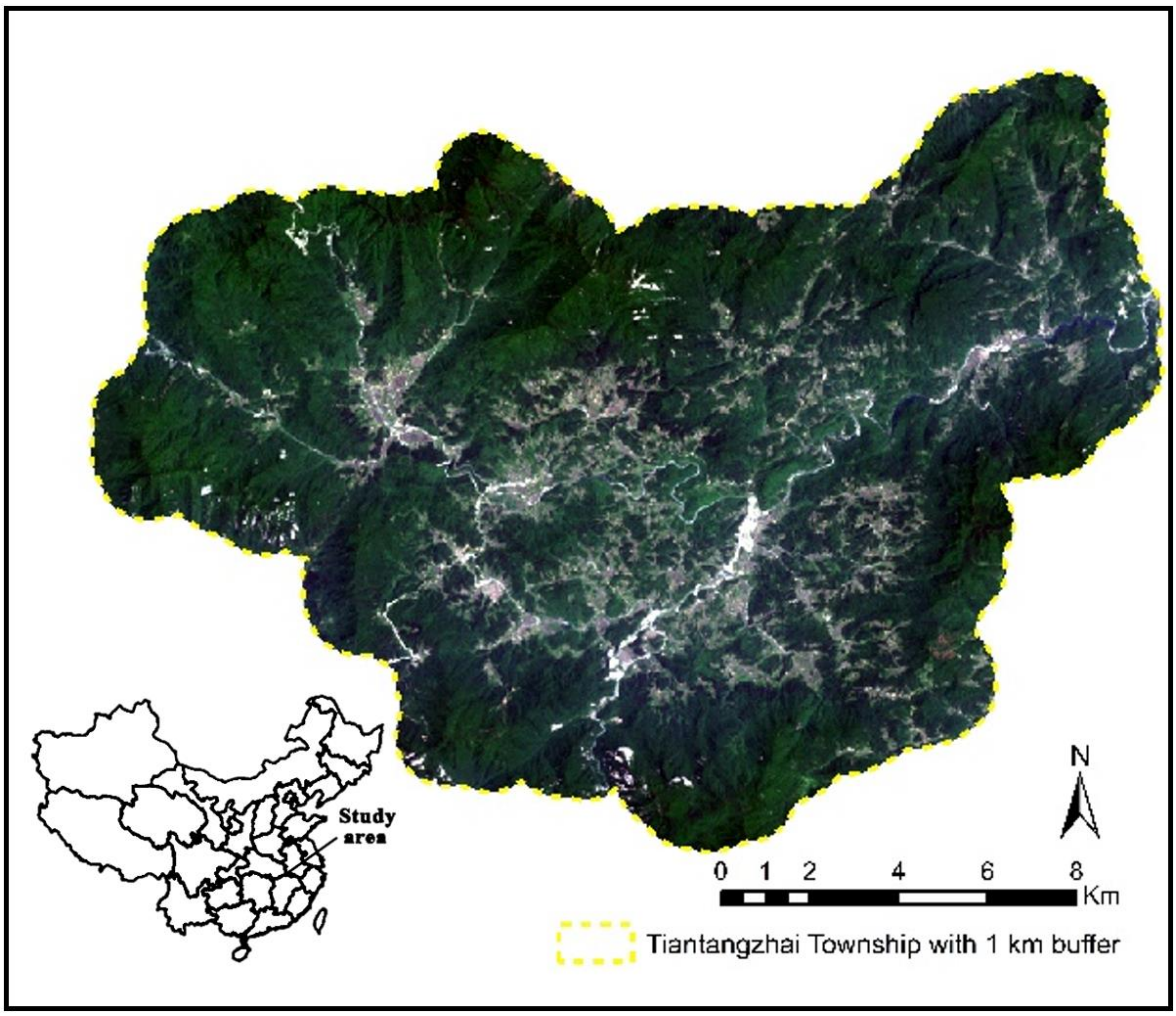

Fig. 1. Study area: Tiantangzhai Township at Jinzhai County Anhui, China

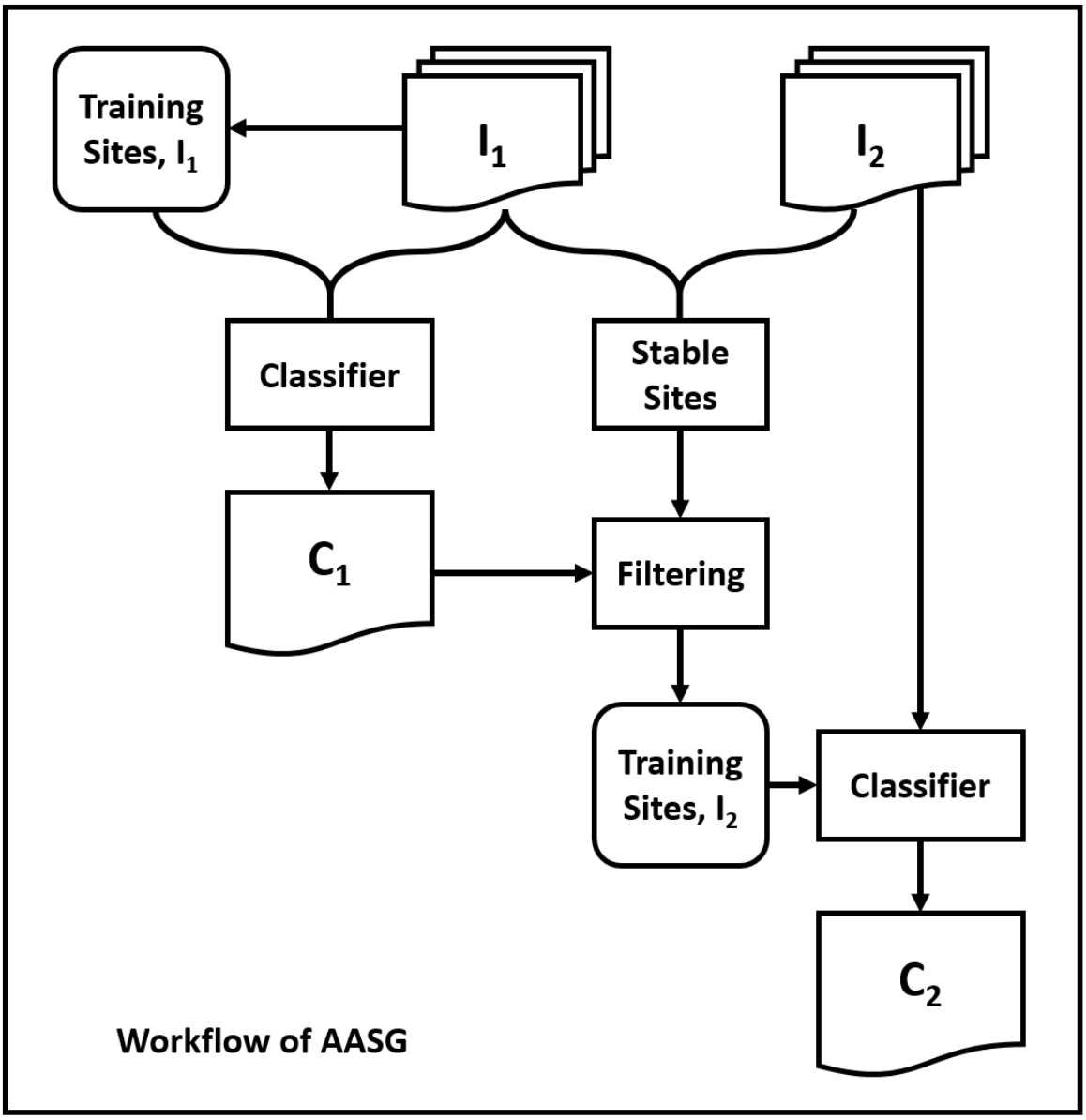

Fig. 2. Fundamentals of the workflows for the AASG method developed by Gray and Song, (2013). The reference image (I_1) was classified by using training data with high quality to produce the classification map (C_1). The training sites for the target image (I_2) was automatically derived from the stable pixels identified by image differencing and then used to generate the classified map (C_2). The stable pixels were spatially filtered to eliminate boundaries at both classes and stable patches with higher confusions.

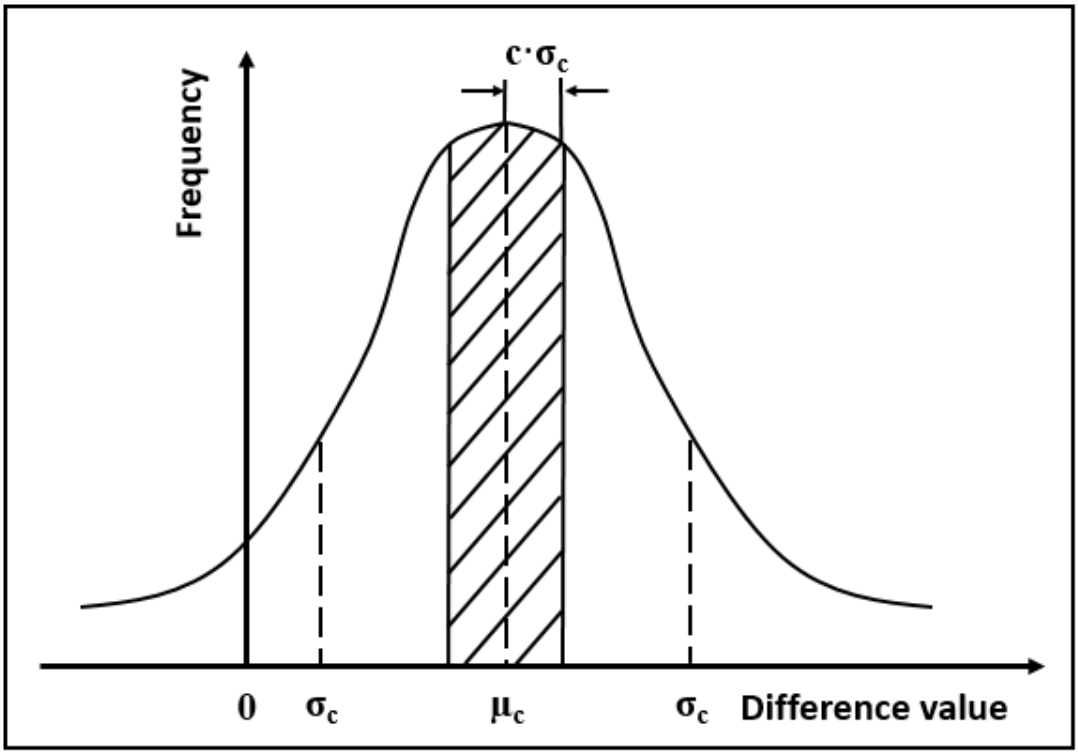

Fig. 3. Selection of *c* parameter for given class. The frequency of the values after subtracting bands for the tow images appears like bell-curve distribution as the image is large enough and the assumption of unchanged of majority pixels holds. The symbols of μ_c, σ_c denotes the mean value and standard deviation of the differencing values. The interval $\mu_c \pm c \cdot \sigma_c$ was chosen in terms of the shaded area which contains 1000 pixels of stable sites. If the total number of stable pixels are less than 1000, the interval would be narrowed down to match that including all those pixels.

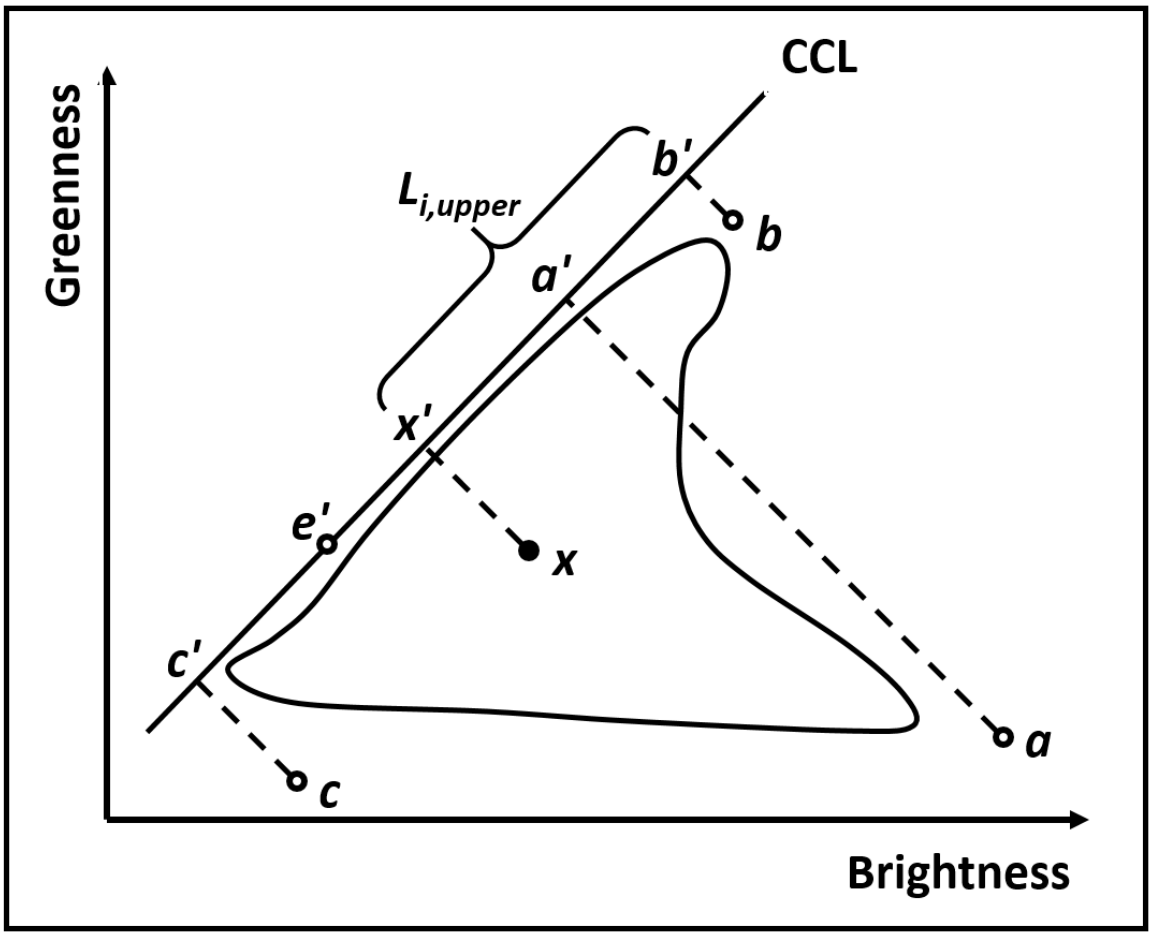

Fig. 4. The B-G space of Tasseled Cap transformation. Point *a* is the pixel with the largest perpendicular distance to the CCL and $d_{max} = |aa'|$. Point *e* (*e'*) is the pixel locates on the CCL (i.e. has the lowest perpendicular distance zero to CCL) and it defines the intercept of CCL. Point c and b defines the upper and lower bound within the length of CCL. $L = |c'b'|$. For the i^{th} pixel x, $d_i = |xx'|$, $L_{i,upper} = |x'b'|$. It should be noted that dmax was lengthened with 10% assuming at least 10% canopy cover given one pixel of forest because the canopy cannot be 0 which means no tree.

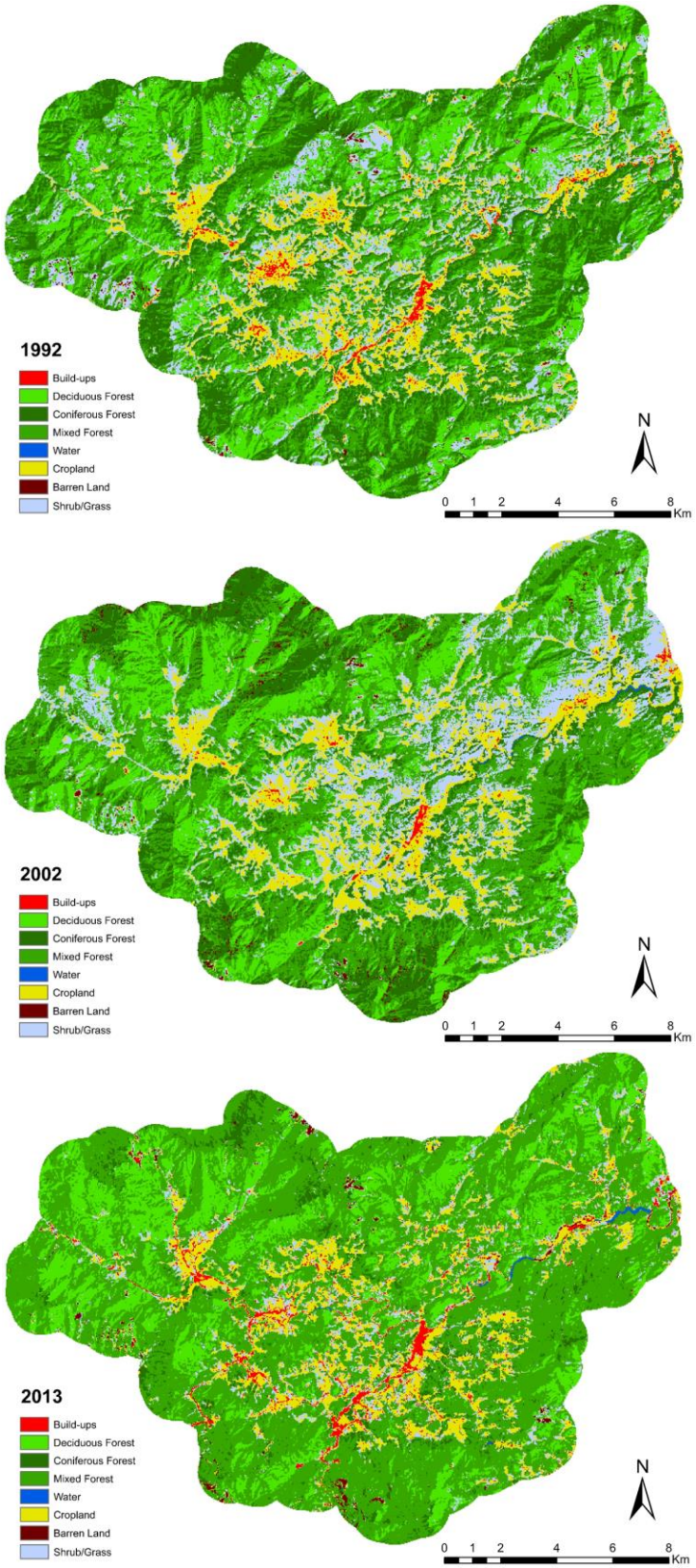

Fig. 5. Land use and land cover in Tiantangzhai Township in 1992, 2002 and 2013

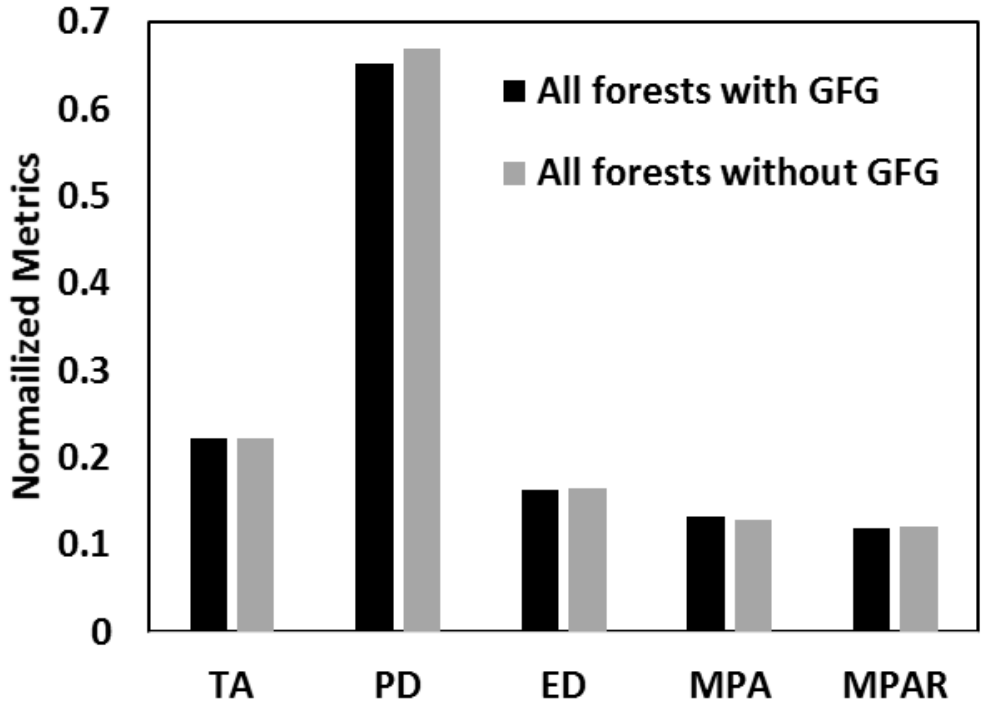

Fig. 6. Changes of landscape metrics for all forests with and without GFG forest stands at the whole region scale. The metrics are normalized to the same scale (0-1) for histogram plotting. Scale, TA: 10^{9}, PD: 10^{-4}, ED: 10^{-1}, MPA: 10^{5}, MPAR: 10^{1}.

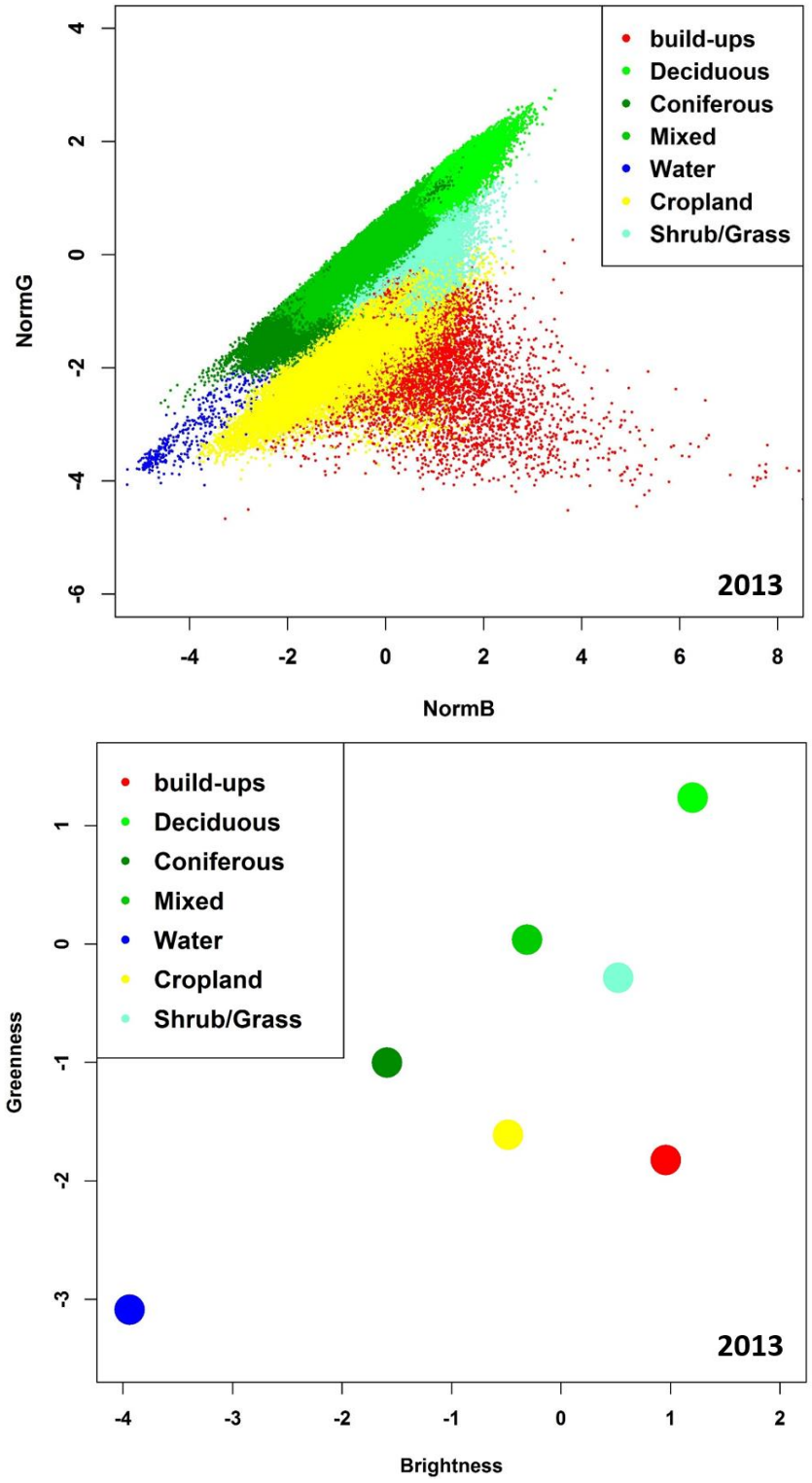

Fig. 7. Scatter plot (above) and spatial distribution of mean values (below) for build-ups, forests (deciduous, coniferous and mixed forest), water, cropland and shrub/grass of Landsat 8 OLI image (2013) in normalized B-G space.

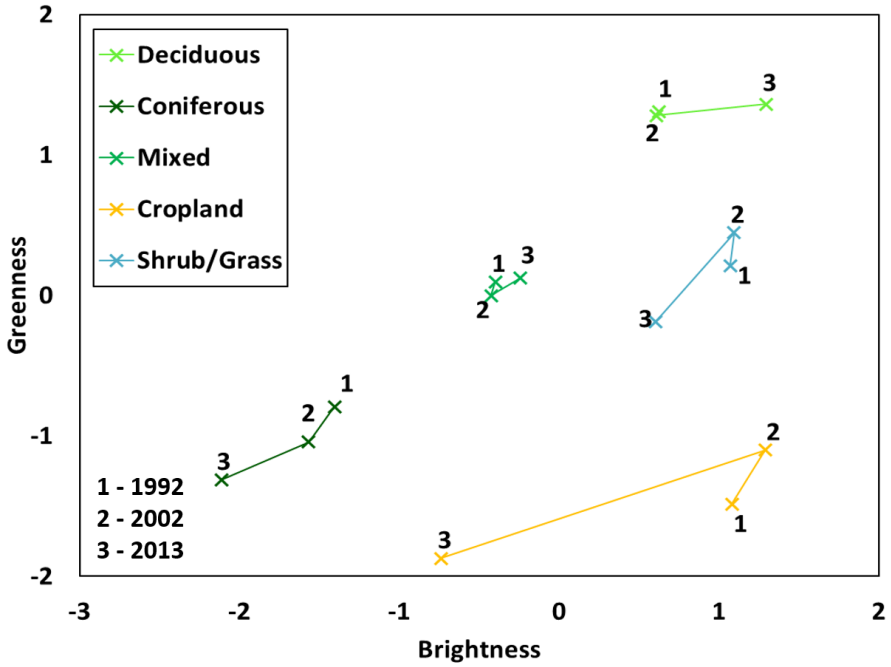

Fig. 8. Temporal trajectories of stable classes in normalized B-G space

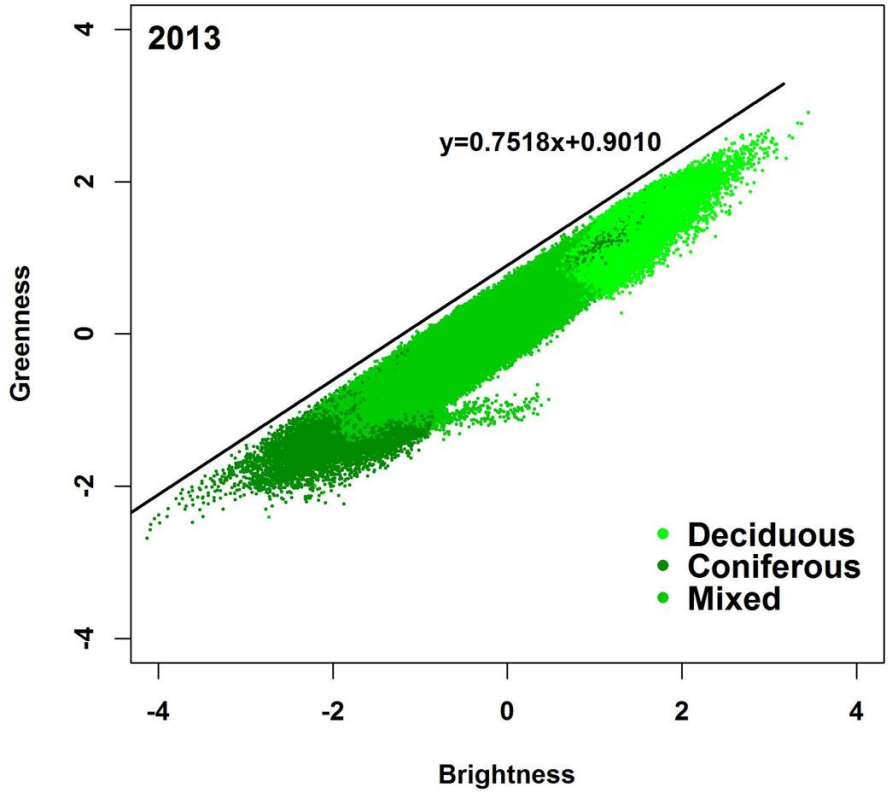

Fig. 9. Scatter plot of forest classes with corresponding canopy closure line (CCL) in 2013

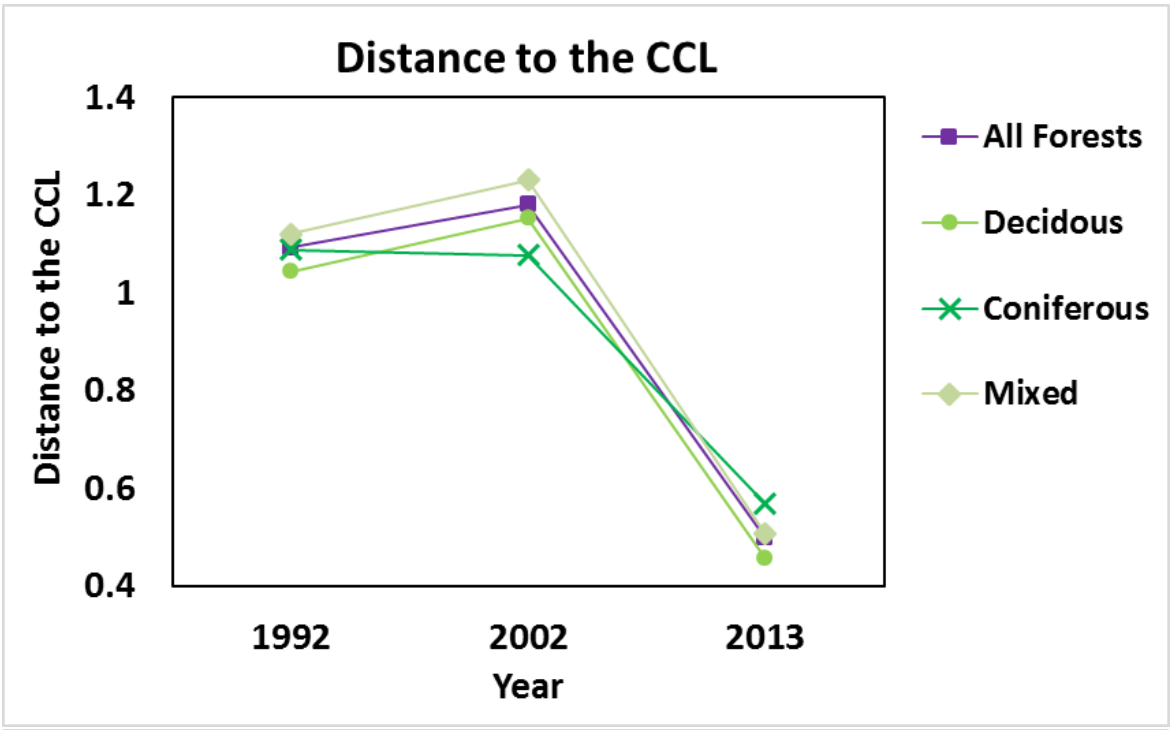

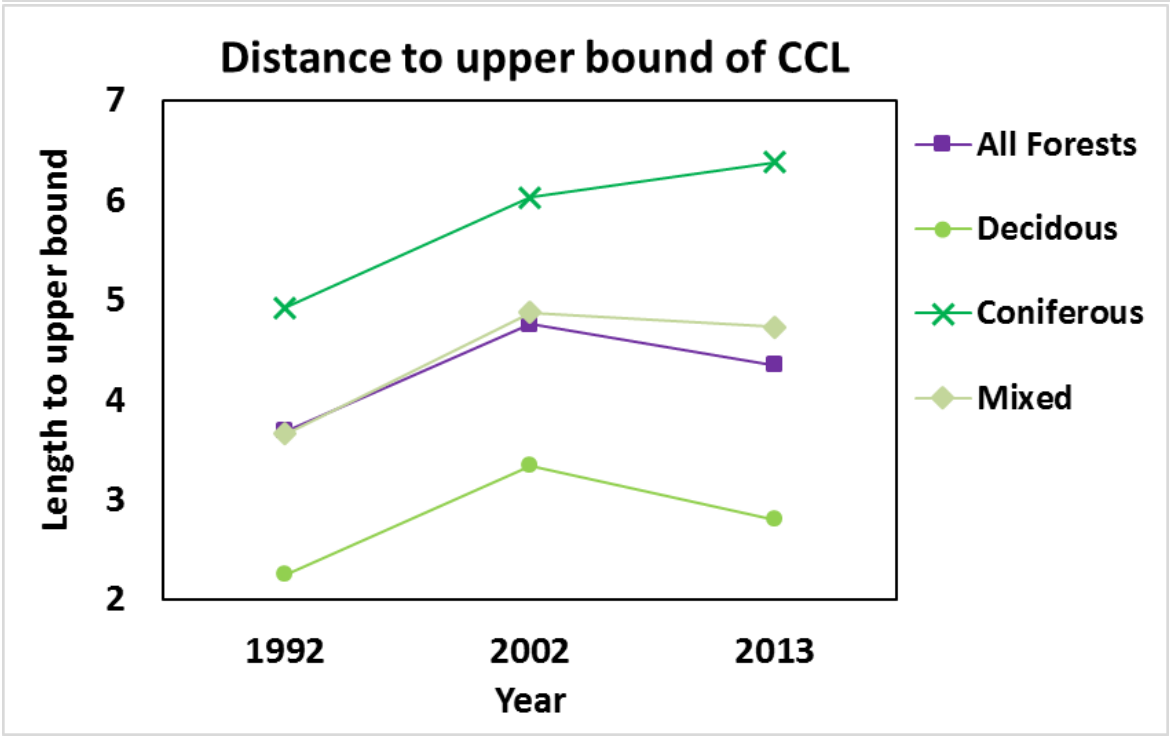

Fig. 10. Temporal change of mean distances to the CCL and $L_{i,upper}$ (distance of vertical point of pixel *i* to the upper bound of CCL)of forest classes (deciduous, coniferous and mixed) and all forests.

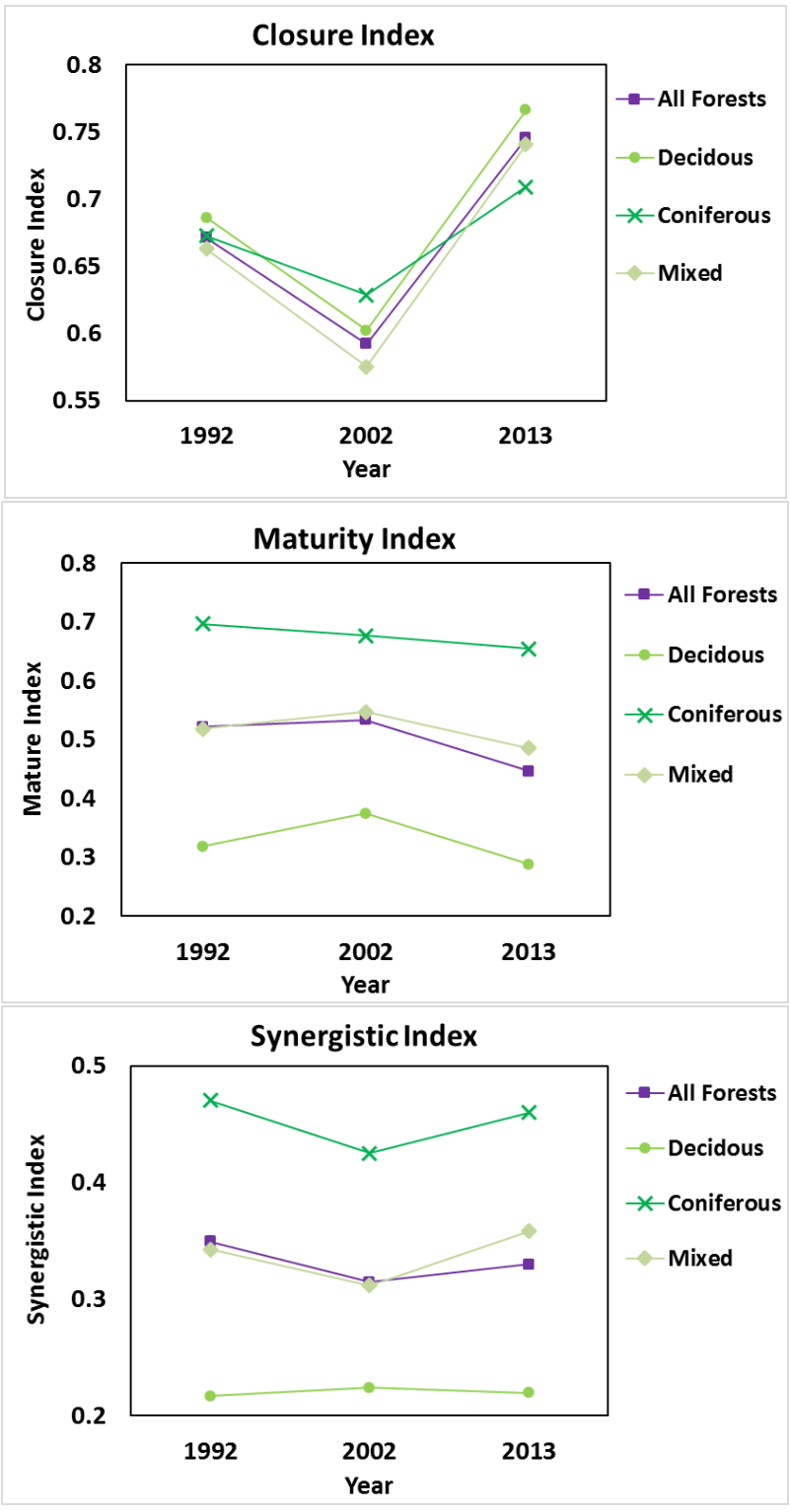

Fig. 11. Temporal change of closure index (CI), maturity index (MI), and synergistic successional index (SynI) of forest classes (deciduous, coniferous and mixed) and all forests

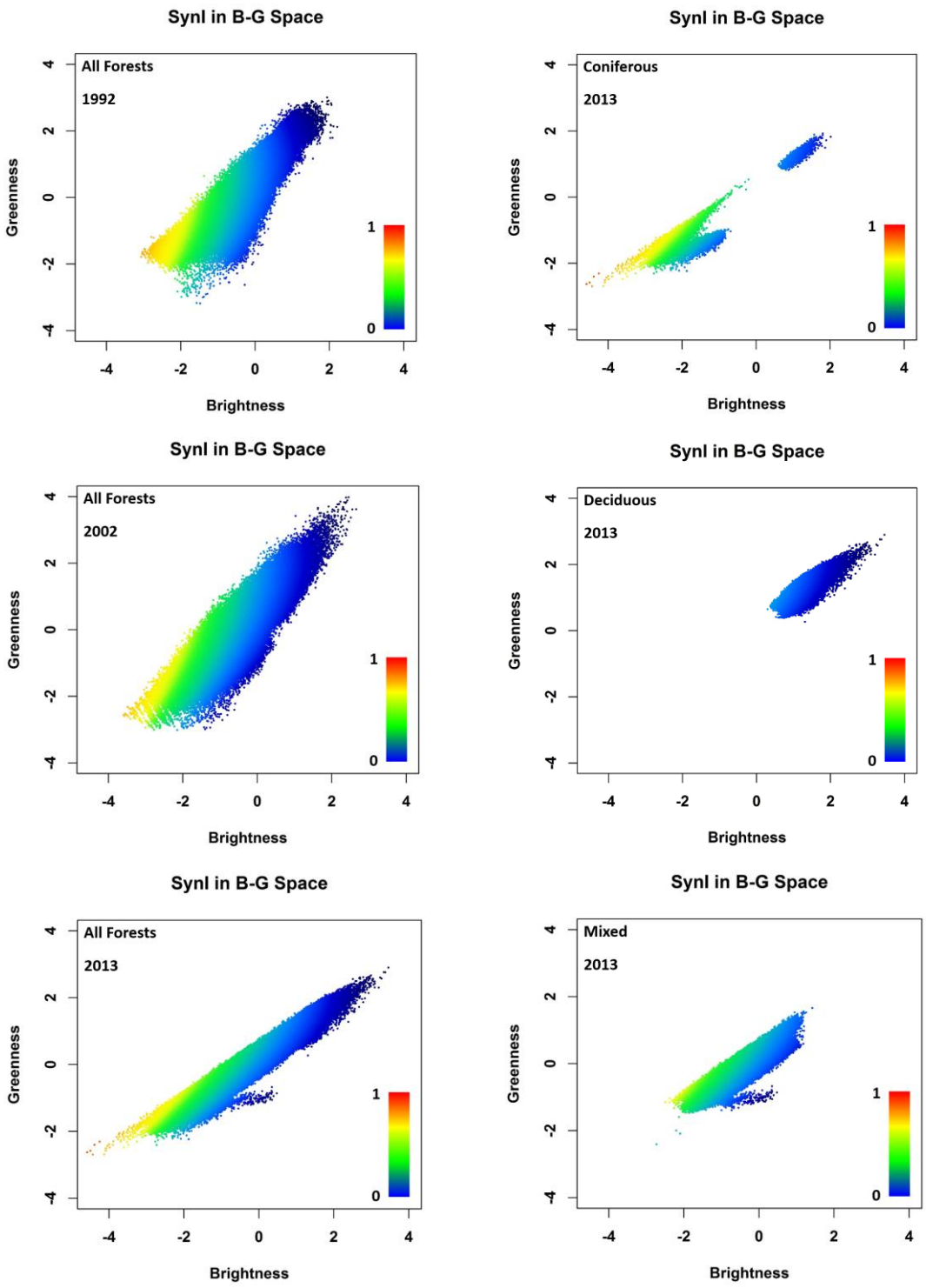

Fig. 12. Scatter plot for SynI. The plots on left display the temporal change (1992, 2002 and 2013) for all the forests. The plots right are illustration of coniferous, deciduous and mixed forest in 2013.

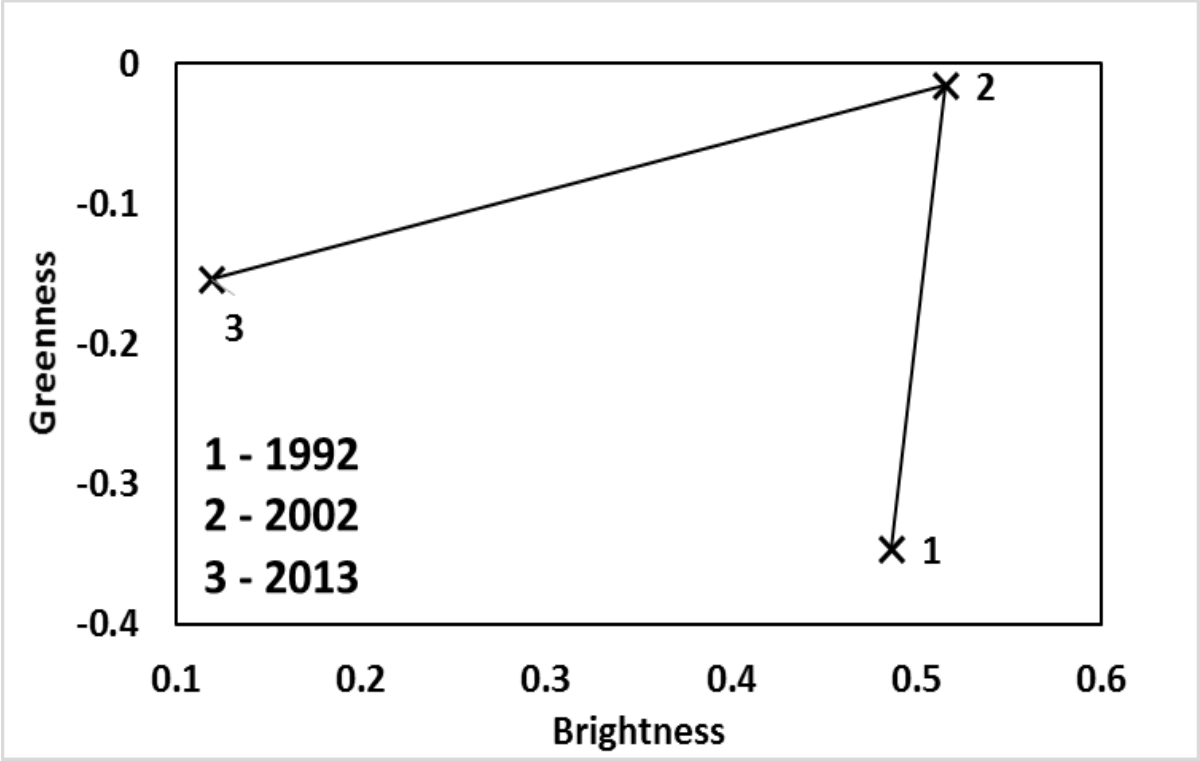

Fig. 13. Temporal trajectory of all GFG forest stands on average in normalized B-G space

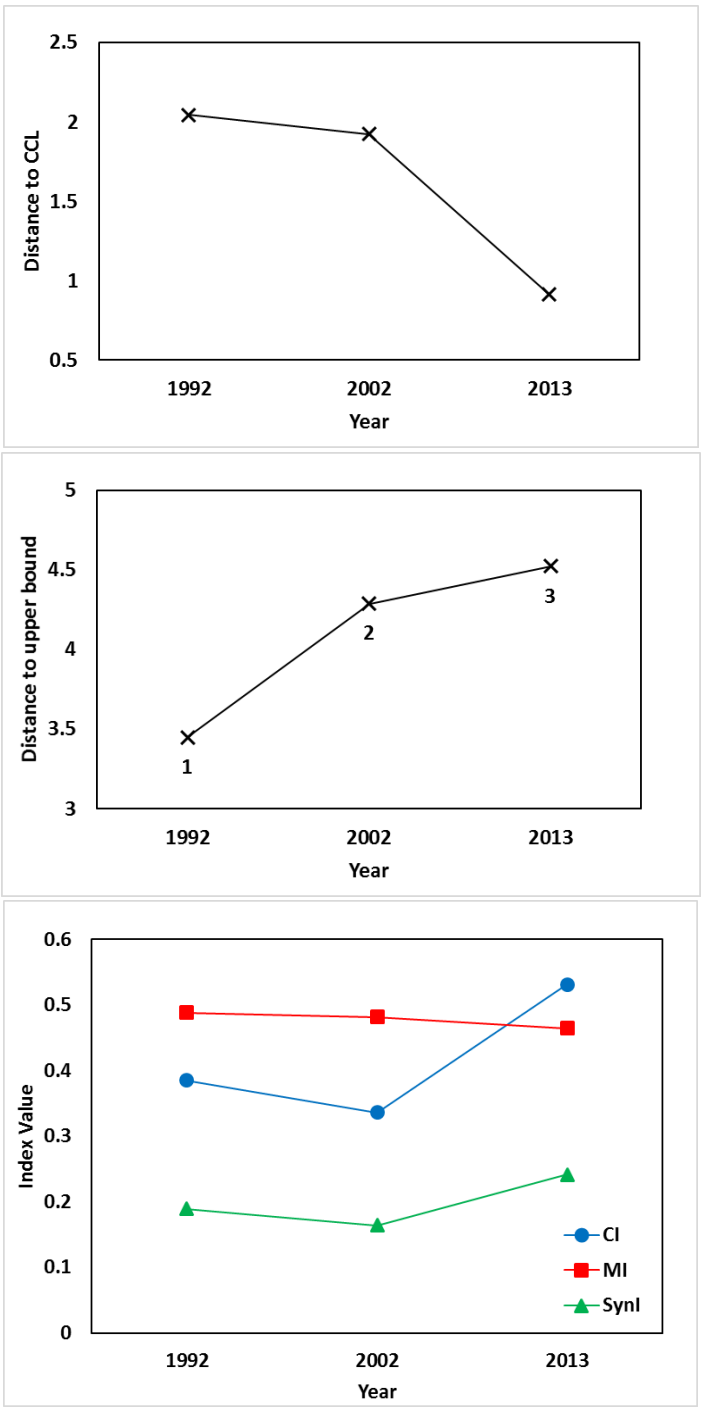

Fig. 14. Temporal change of d_i, $L_{i,upper}$ and CI, MI, SynI on average for GFG forest stands.

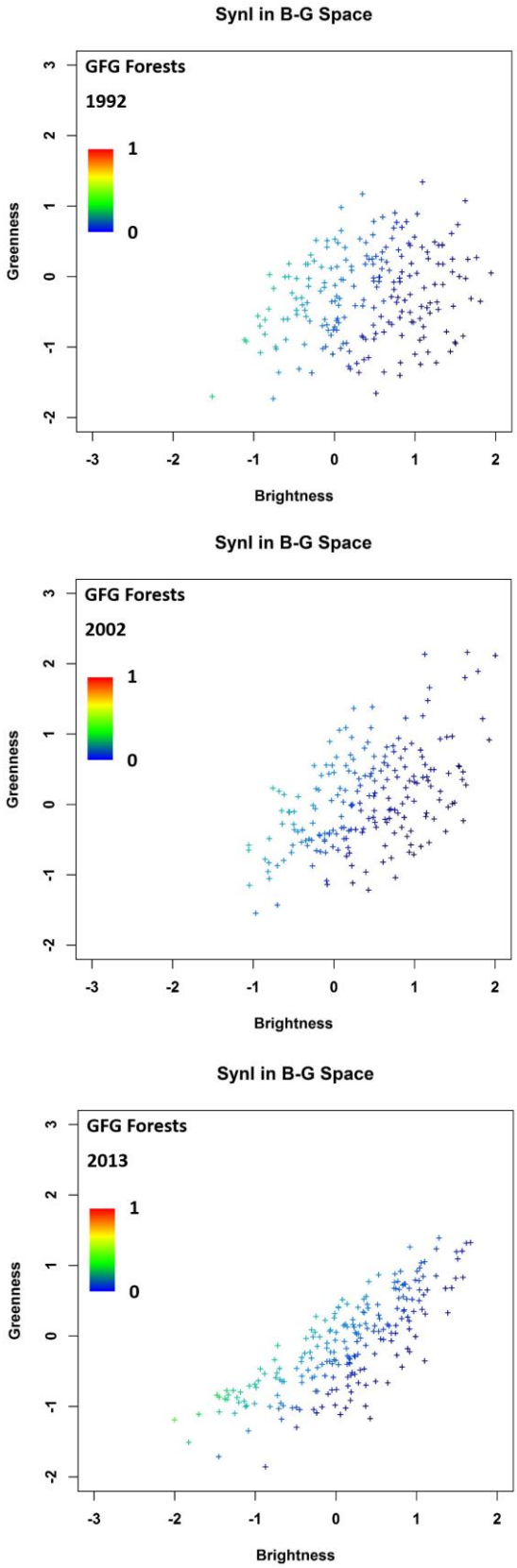

Fig. 15. Scatter plot for SynI of all the GFG forest stands in 1992, 2002, and 2013

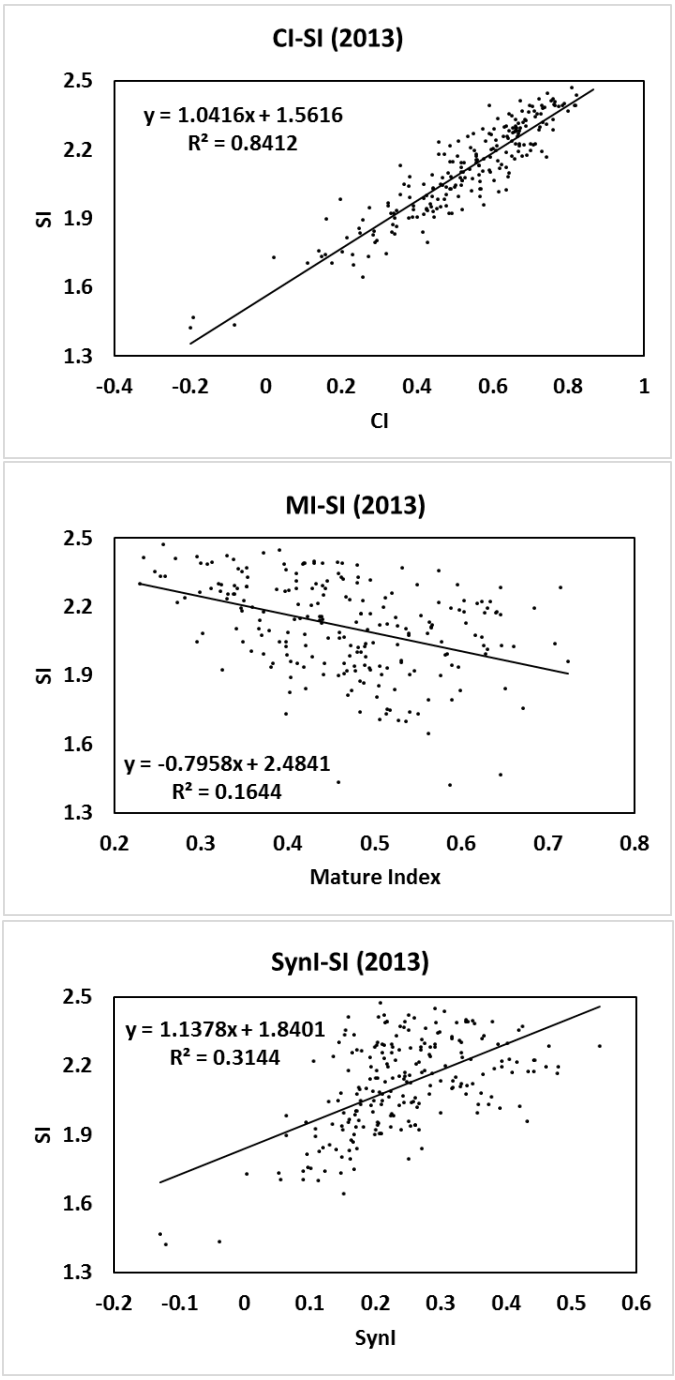

Fig. 16. Correlations of CI, MI, SynI with structural index (SI) of GFG forest stands in 2013

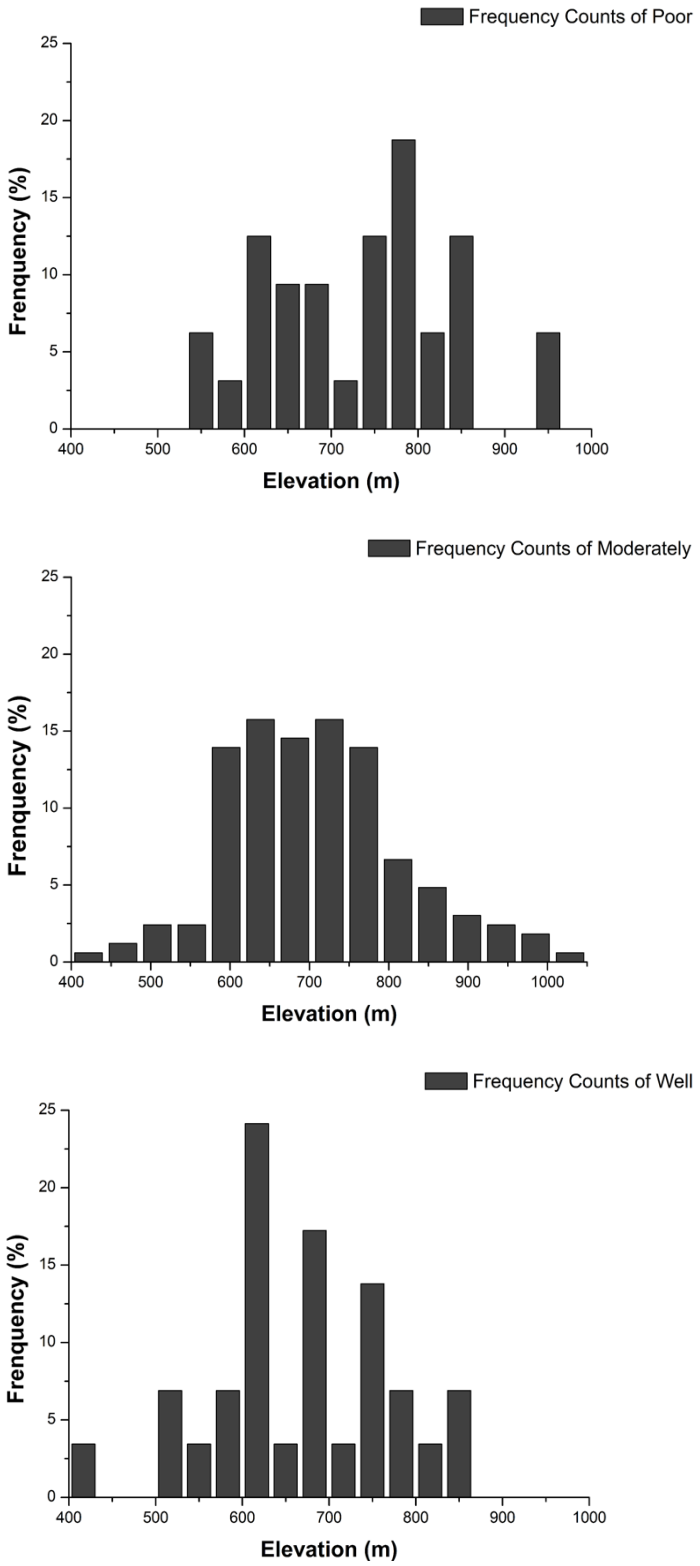

Fig. 17a. Proportional distribution of mean elevation of GFG forest stands for different levels of growing trend based on the change of SynI between 2002 and 2013.

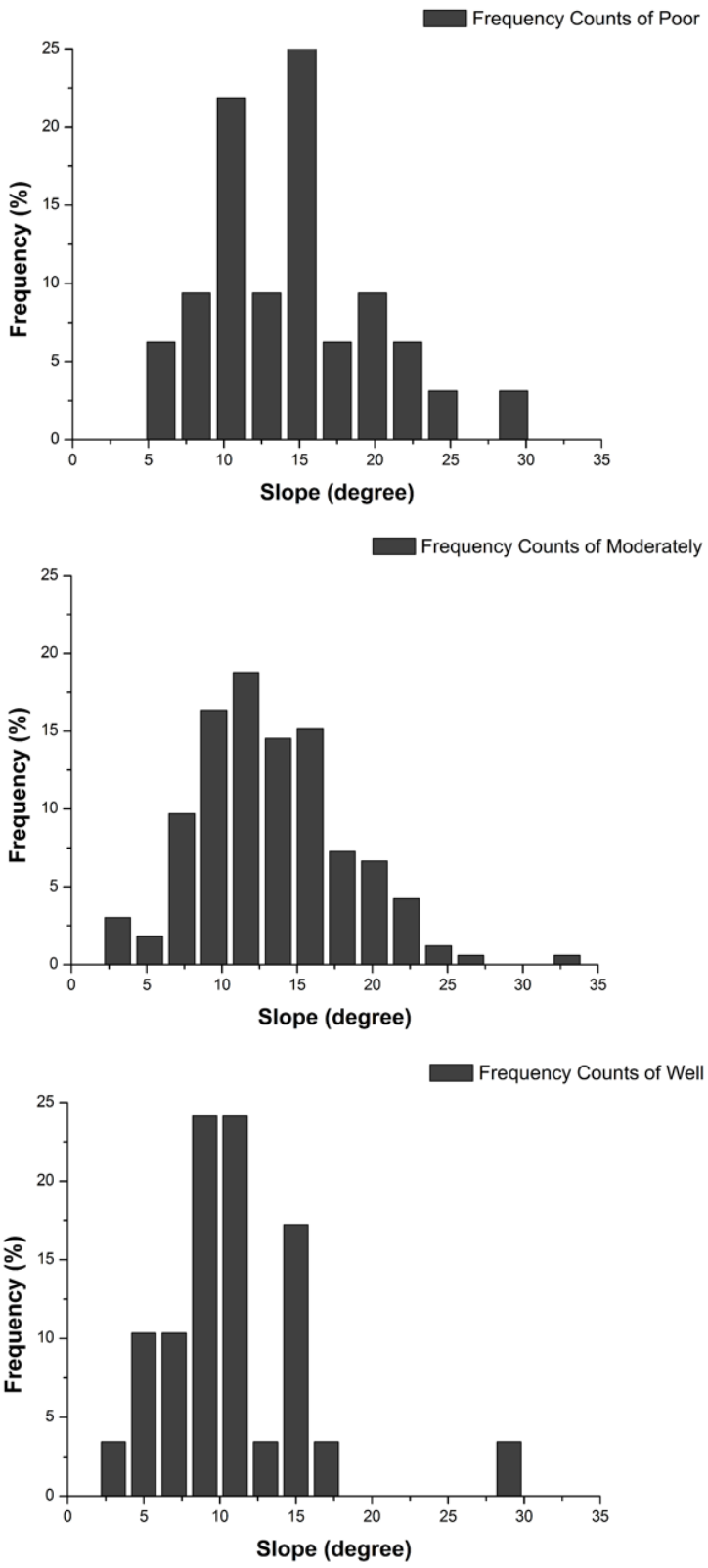

Fig. 17b. Proportional distribution of mean slope of GFG forest stands for different levels of growing trend based on the change of SynI between 2002 and 2013.

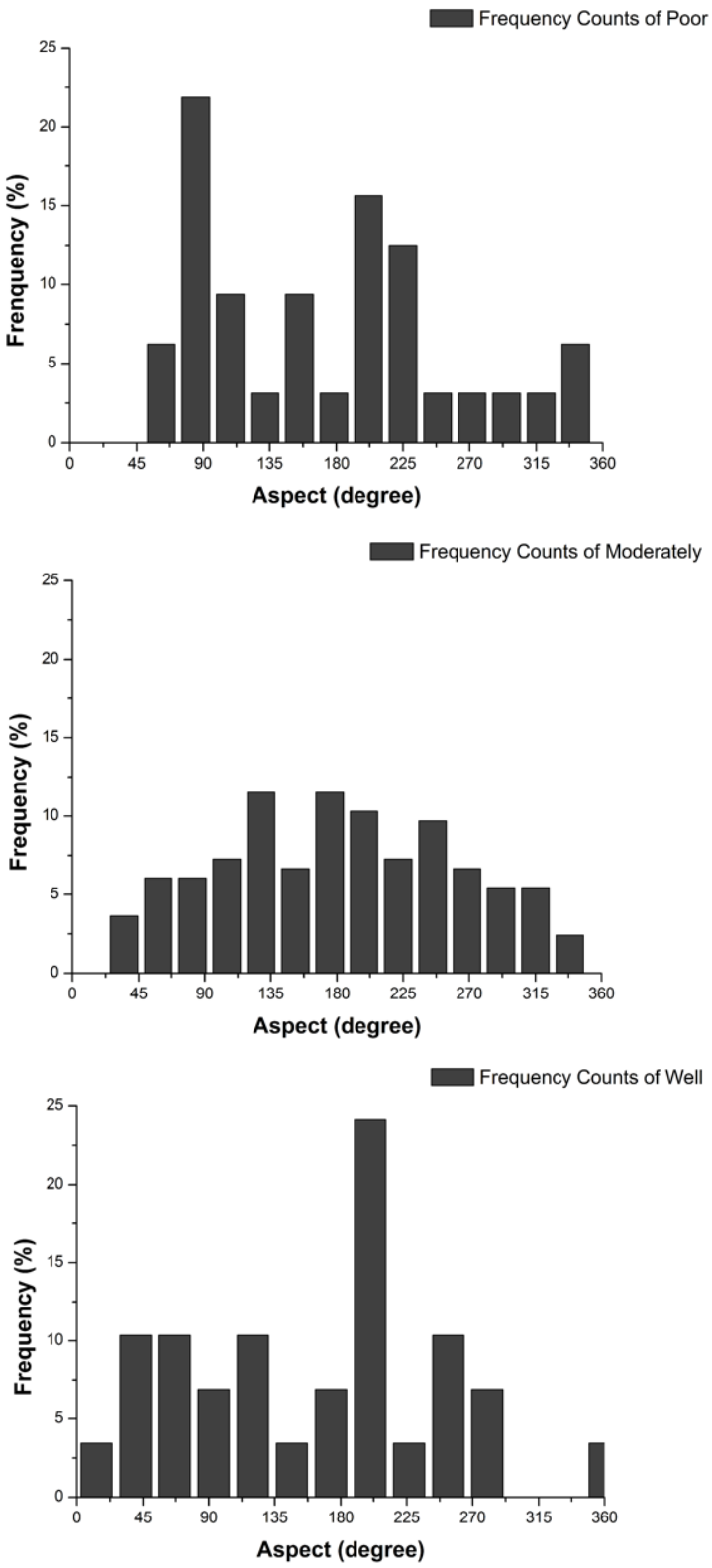

Fig. 17c. Proportional distribution of mean slope of GFG forest stands for different levels of growing trend based on the change of SynI between 2002 and 2013.

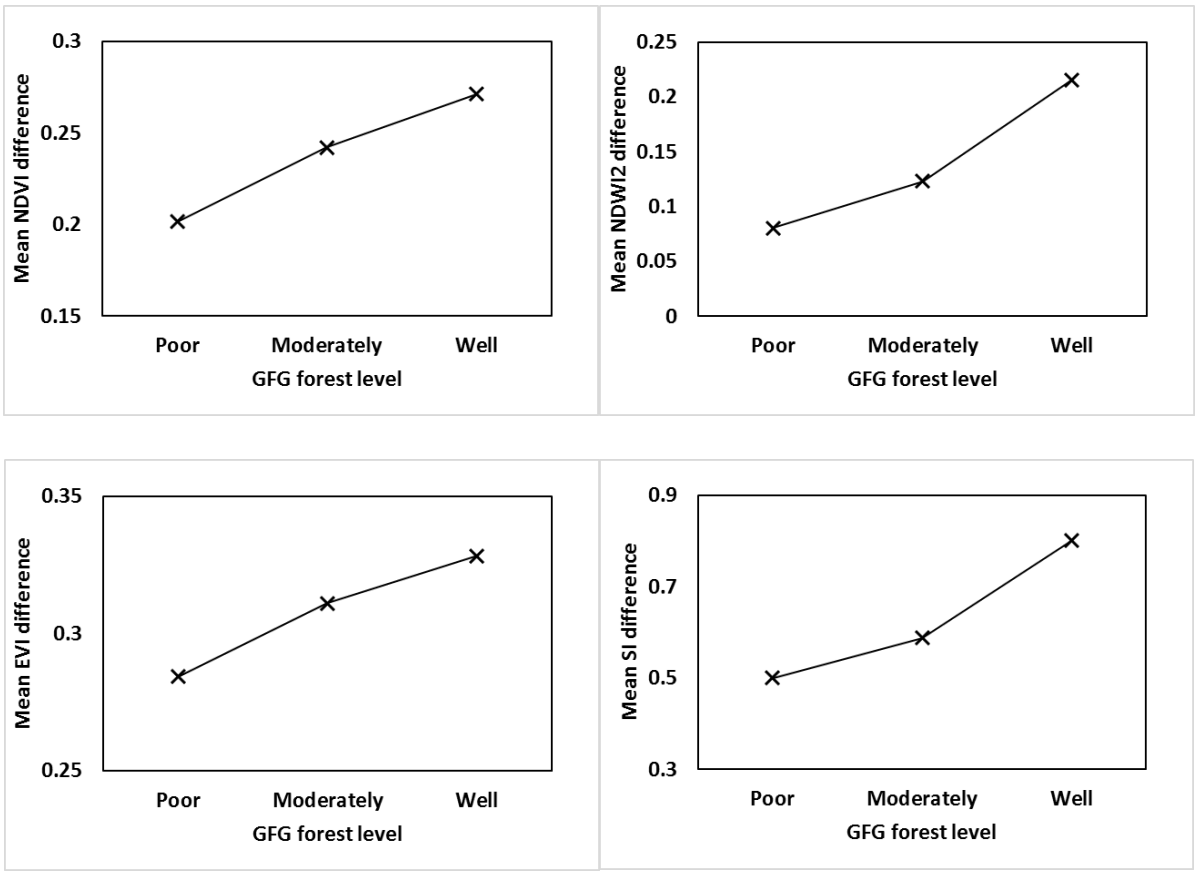

Fig. 18. Vegetation index (NDVI, NDWI2, EVI, and SI) difference for the three levels of GFG forest based on the change of SynI between Year 2002 and 2013.

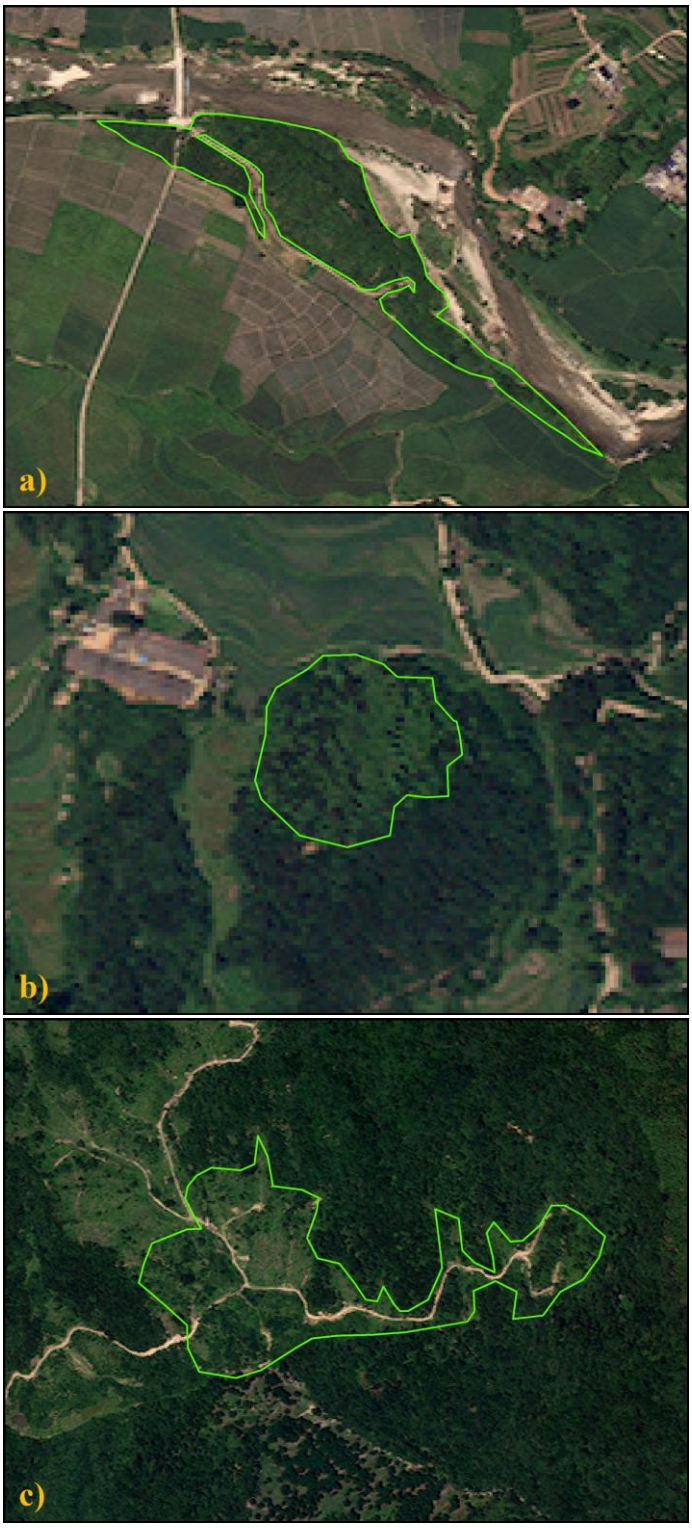

Fig. 19. Illustrations of GFG forest stands at levels of a) well-, b) moderately- and c) poor development for growth trend based on the change of SynI between 2002 and 2013. The green polygons represent the boundary of the forest stands over the fine spatial resolution image of WorldView-2 satellite.

REFERENCES

Archer, K.J., Kimes, R.V., 2008. Empirical characterization of random forest variable importance measures. *Computational Statistics & Data Analysis*. 52, 2249–2260.

Beven. K.J. and Kirkby. M.J., 1979. A physically-based variable contributing area model of basin hydrology. *Hydrological Sciences Bulletin*, 24, 43–69.

Breiman, L., 1999. Random forests-random features. Technical Report 567, Statistics Department, University of California, Berkeley.

Briem, G. J., Benediktsson, J. A. and Sveinsson, J. R., 2002. Multiple classifiers applied to multisource remote sensing data. *IEEE Transactions on Geoscience and Remote Sensing*, 40, 2291-2299.

Butchart, S. H. M., Walpole, M., Collen, B., van Strien, A., Scharlemann, J. P. W., Almond, R. E. A., et al., 2010. Global biodiversity: Indicators of recent declines. *Science*, 328, 1164–1168.

Caspersen, J.P., Pacala, S.W., Jenkins, J.C., Hurtt, G.C., Moorcroft, P.R., and Birdsey, R.A., 2000. Contributions of land-use history to carbon accumulation in U.S. forests. *Science*, 290, 1148–1151.

Charney, J. and Stone, P.H., 1975. Drought in the Sahara: A biogeophysical feedback mechanism. *Science*, 187, 434–435.

Chavez, P. S., Jr., 1996, Image-based atmospheric corrections revisited and improved. *Photogrammetric Engineering and Remote Sensing*, 62, 1025–1036.

Chen, X., Lupi, F., Li, A., Sheely, R., Vina, A., and Liu, J., 2012. Agent-based modeling of the effects of social norms on enrollment in payments for ecosystem services. *Ecological Modeling*, 229, 16–24.

Chen, X., Lupi, F., Vina, A., He, G., and Liu, J., 2010. Using cost-effective targeting to enhance the efficiency of conservation investments in payments for ecosystem services. *Conservation Biology*, 24, 1469–1478.

China State Council, 2000. Guidelines on Further Implementation of Returning Cropland to Forests/Grassland. State Council 2000, No. 24.

CIFOR REHAB, 2003. Review of Forest Rehabilitation Initiatives website, http://www.cifor.cgiar.org/rehab.

Cohen, A.L., Singhakumara, B.M.P. and Ashton, P.S., 1995. Releasing rain forest succession: a case study in the Dicranopteris linearis fernlands of Sri Lanka. *Restoration Ecology*, 3, 261–270.

Cutler, A., and Stevens, J.R., 2006. Random forests for microarrays. *Methods in Enzymology*, 411, 422–432.

Dale, V.H., Brown, S., Haeuber, R.A., Hobbs, N.T., Huntly, Naiman, R.J., Riebsame, W. E., Turner, M. G. and Valone, T. J., 2000. Ecological Principles and Guidelines for Managing the Use of Land. *Ecological Applications*, 10, 639–670.

Deng, H., Zheng, P., Liu, T. and Liu, X., 2011. Forest ecosystem services and eco-compensation mechanisms in China. *Environmental Management*, 48, 1079–1085.

Dietterich, T.G., 2002. Ensemble Learning. The handbook of brain theory and neural networks, M.A. Arbib (Ed.) (Cambridge, MA: The MIT Press).

Dixon R.K., Brown S., Houghton R.A., Solomon A.M., Trexler M.C., Wisniewski J., 1994. Carbon pools and flux of global forest ecosystems. *Science*, 263, 185–190.

Dobson, A.P., Bradshaw, A.D., and Baker, A.J.M., 1997. Hopes for the future: restoration ecology and conservation biology. *Science*, 277, 515–522.

Durst, P.B., Waggener, T.R., Enters, T., and Cheng, T.L., 2001. Forests out of bounds: impacts and effectiveness of logging bans in natural forests in Asia-Pacific. FAO, Bangkok.

Fiorella, M. and Ripple, W.J., 1993a. Determining successional stage of temperate coniferous forests with Landsat satellite data. *Photogrammetric Engineering and Remote Sensing*, 59, 239–246.

Fiorella, M., and Ripple, W.J., 1993b. Analysis of conifer regeneration using Landsat Thematic Mapper data. *Photogrammetric Engineering and Remote Sensing*, 59, 1383–1388.

Fischer, J., Hartel, T., & Kuemmerle, T., 2012. Conservation policy in traditional farming landscapes. *Conservation Letters*, 5, 167–175.

Gao, B.G., 1996. NDWI-a normalized difference water index for remote sensing of vegetation liquid water from space. *Remote Sensing of Environment*, 58, 257-266.

Gauvin, C., Uchida, E., Rozelle, S., and Xu, J., 2010. Cost-effectiveness of payments for ecosystem services with dual goals of environment and poverty alleviation. *Environmental Management*, 45, 488–501.

Gemmell, F.M., 1995. Effects of forest cover, terrain, and scale on timber estimation with Thematic Mapper data in a Rocky Mountain site. *Remote Sensing of Environment*, 51, 291–305.

Gemmell, F., and Varjo, J., 1999. Utility of reflectance model inversion versus two spectral indices for estimating biophysical characteristics in a boreal forest test site. *Remote Sensing of Environment*, 68, 95–111.

Geri, F., Amici, V., and Rocchini, D., 2010. Human activity impact on the heterogeneity of a Mediterranean landscape. *Applied Geography*, 29, 1–10.

Giacinto, G. and Roli, F. (1997) Adaptive selection of image classifiers. In Proc. ICIAP (Springer Verlag Lecture Notes in CS Vol. 1310), pp. 38–45

Gray, J. and Song, C., 2013. Consistent classification of image time series with automatic adaptive signature generalization. *Remote Sensing of Environment*, 134, 333–341.

Helmer, E. H., Brown, S., and Cohen, W. B., 2001. Mapping montane tropical forest successional stage and land use with multi-date Landsat imagery. *International Journal of Remote Sensing*, 21, 2163–2183.

Hu, C.X., Fu, B.J., Chen, L.D. and Gulinck. H., 2006. Farmer's attitudes towards Grain-for-Green program in the Loess hilly area, China – a case study in two small catchments. *International Journal of Sustainable Development and World Ecology*, 13, 211–220.

Huete, A.R., Liu, H.Q., Batchily, K., and van Leeuwen, W.J.D., 1997. A comparison of vegetation indices over a global set of TM images for EOS-MODIS. *Remote Sensing of Environment*, 59, 440–451.

Jiang, Z.Y., Huete, A.R., Didan, K. and Miura, T., 2008. Development of a two-band enhanced vegetation index without a blue band. *Remote Sensing of Environment*, 112, 3833–3845.

Jordan, C.F., 1969. Derivation of leaf-area index from quality of light on forest floor. *Ecology*, 50, 663–667.

Kauth, R., and Thomas, G., 1976. The tasseled-cap – a graphic description of the spectral-temporal development of agricultural crops as seen by Landsat. Machine Processing of Remotely Sensed Data, Symposium Proceedings. Purdue University/LARS, West Lafayette, iN. In:Cicone, R.C. and M.D. Metzler. 1984. Comparison of Landsat MSS, Nimbus-7 CZCS, and NOAA-7 AVHRR features for land-use analysis. *Remote Sensing of Environment*, 14, 257–265.

Leitão, A. B., and Ahern, J., 2002. Applying landscape ecological concepts and metrics in sustainable landscape planning. *Landscape and Urban Planning*, 59, 65–93.

Lelieveld, J., 2010. Atmospheric chemistry: A missing sink for radicals. *Nature*, 466, 925–926.

Li, H., Ma, Y., Aide, T.M. and Liu, W., 2008. Past, present and future land-use in Xishuangbanna, China and the implications for carbon dynamics. *Forest Ecology and Management*, 255, 16–24.

Li, Y., Viña, A., Yang, W., Chen, X., Zhang, J., Ouyang, Z., Liang, Z. and Liu, J., 2013. Effects of conservation policies on forest cover change in panda habitat regions, China. *Land Use Policy*, 33, 42–53.

Lucas, R.M., Honzak, M., do Amaral, I., Curran, P.J. and Foody, G.M., 2002. Forest regeneration on abandoned clearances in central Amazonia. *International Journal of Remote Sensing*, 23, 965–988.

McFeeters, S.K., 1996. The use of the Normalized Difference Water Index (NDWI) in the delineation of open water features. *International Journal of Remote Sensing*, 17, 1425−1432.

Meyer, W.B., 1995. Past and present land use and land cover in the USA. *Consequences*, 1, 25–33.

Millán, V.E.G., Arturo Sánchez Azofeifa, G., Malvárez, G.C., Moré, G., Pons, X. and Yamanaka-Ocampo, M., 2013. Effects of topography on the radiometry of CHRIS/PROBA images of successional stages within Tropical Dry Forests. *IEEE Journal of Selected Topics in Applied Earth Observations and Remote Sensing*, 6, 1584−1595.

Millennium Ecosystem Assessment, M. A., 2005. Ecosystems and human well-being: Synthesis. Washington, DC: World Resources Institute.

Moran, M.S., Jackson, R.D., Slater, P.N. and Teillet, P. M., 1992. Evaluation of simplified procedures for retrieval of land surface reflectance factors from satellite sensor output. *Remote Sensing of Environment*, 41, 169–184.

Mullan, K., Kontoleon, A., Swanson, T., and Zhang, S., 2010. Evaluation of the impact of the Natural Forest Protection Program on rural household livelihoods. *Environmental Management*, 45, 513–525.

Myneni R.B., Dong J., Tucker C.J., Kaufmann R.K., Kauppi P.E., Liski J., et al. A large carbon ink in the woody biomass of northern forests. *Proceedings of the National Academy of Sciences*, 2001a, 14784–14789.

Otterman, J., 1974. Baring high-albedo soils by overgrazing: a hypothesised desertification mechanism. *Science*, 86, 531–533.

Pal, M., 2005, Random forest classifier for remote sensing classification. *International Journal of Remote Sensing*, 26, 217–222.

Pan, Y. et al., 2011. A large and persistent carbon sink in the world's forests. *Science*, 333, 988–993.

Pax-Lenney, L. M., Woodcock, C. E., Macomber, S. A., Gopal, S., and Song, C., 2001. Forest mapping with a generalized classifier and Landsat TM data. *Remote Sensing of Environment*, 77, 241–250.

Persha, L., Agrawal, A., and Chhatre, A., 2011. Social and ecological synergy: local rulemaking, forest livelihoods, and biodiversity conservation. *Science*, 331, 1606–1608.

Prasad A.M., Iverson L.R., Liaw A., 2006. Newer classification and regression tree techniques: bagging and random forests for ecological prediction. *Ecosystems*, 9, 181–199.

Ribeiro, S. C., and Lovett, A., 2009. Associations between forest characteristics and socio-economic development: a case study from Portugal. *Journal of Environmental Management*, 90, 2873–2881.

Pregitzer, K.S. and Euskirchen, E.S., 2004. Carbon cycling and storage in world forests: biome patterns related to forest age. *Global Change Biology*, 10, 2052–2077.

Rouse, J.W., Haas, R.H., Schell, J.A. and Deering, D.W., 1973. Monitoring vegetation systems in the Great Plains with ERTS. In S. C. Freden, E. P. Mercanti, and M. A. Becker (Eds.), Third earth resources technology satellite–1 Symposium–Volume I: Technical presentations.

Running S.W., Nemani R.R., Peterson D.L., Band L.E., Potts D.F., Pierce L.L., Spanner M.A., 1989. Mapping regional forest evapotranspiration and photosynthesis by coupling satellite data with ecosystem simulation. Ecology, 70, 1090–1101.

Sagan, C. et al. 1979. Anthropogenic albedo changes and the Earth's climate. *Science*, 206, 1363–1368.

Salim, E., and Ullsten, O., 1999. Our Forests our Future. Cambridge University Press, Cambridge, UK.

Serra, P., Pons, X., Saurí, D., 2008. Land-cover and land-use change in a Mediterranean landscape: A spatial analysis of driving forces integrating biophysical and human factors. *Applied Geography*, 28, 189–209.

Shen, Y., Liao, X. and Yin, R., 2006. Measuring the socioeconomic impacts of China's Natural Forest Protection Program. *Environmental and Development Economics*, 11, 769–788.

Sieber, A., Kuemmerle, T., Prishchepov, A.V., Wendland, K.J., Baumann, M., Radeloff, V.C., Baskin, L.M., and Hostert, P., 2013. Landsat-based mapping of post-Soviet land-use change to assess the effectiveness of the Oksky and Mordovsky protected areas in European Russia. *Remote Sensing of Environment*, 133, 38–51.

Song, C. and Woodcock, C. E., 2003. A regional forest ecosystem carbon budget model: Impacts of forest age structure and landuse history. *Ecological Modelling*, 164, 33−47.

Song, C., Woodcock, C.E., and Li, X., 2002. The spectral/temporal manifestation of forest succession in optical imagery: The potential of multitemporal imagery. *Remote Sensing of Environment*, 82, 282–289.

Song, C., Schroeder, T.A., and Cohen, W.B., 2007. Predicting temperate conifer forest successional stage distributions with multiple Landsat Thematic Mapper imagery. *Remote Sensing of Environment*, 106, 228–237.

Song. C., Zhang, Y., Mei, Y., Liu, H., Zhang, Z., Zhang, Q., Zha, T., Zhang, K., Huang, C., Xu, X., Jagger, P., Chen, X. and Bilsborrow, R., 2013. Sustainability of forests created by china's sloping land conversion program: a comparison among three sites in Anhui, Hubei and Shanxi. *Forest Policy and Economics*, 38, 161–167.

Su, S.L., Jiang, Z.L., Zhang, Q. and Zhang, Y., 2011. Transformation of agricultural landscapes under rapid urbanization: a threat to sustainability in Hang-Jia-Hu region, China. *Applied Geography*, 31, 439–449.

Tong, S.T.Y. and Chen, W.L., 2002. Modeling the relationship between land use and surface water quality. *Journal of environmental management*, 66, 377–393

Turner, M.G., Gardner, R.H. and O'Neill, R.V., 2001. Landscape Ecology: in Theory and Practice. Springer-Verlag, New York.
Song, C., Woodcock, C.E., and Seto, K.C., 2001. Classification and change detection using Landsat TM data: when and how to correct atmospheric effects? *Remote Sensing of Environment*, 75, 230–244.

Wang, C., Ouyang, H., Maclaren, V., Yin, Y., Shao, B., Boland, A., Tian, Y., 2007. Evaluation of the economic and environmental impact of converting cropland to forst: a case study in Dunhua county, *China. Journal of Environmental Management*, 85, 746–756.

Weyerhaeuser, H., Wilkes, A., and Kahrl, F., 2005. Local impacts and responses to regional forest conservation and rehabilitation programs in China's northwest Yunnan province. Agricultural Systems, 85, 234–253.

WRI (World Resources Institute), 2003. World Resources Report 2002–2004: Decisions for the Earth: Balance, Voice, and Power. World Resources Institute, Washington, DC.

Zhang, P., Shao, G., Zhao, G., Le Master, D., Parker, G., Dunning, J. and Li, Q., 2000. China’s forest policy for the 21st century. *Science*, 288, 2135–2136.